(12)

AD-A160 797

AD

US ARMY
MATERIEL
COMMAND

TECHNICAL REPORT BRL-TR-2678

REFLECTED IMPULSE NEAR SPHERICAL CHARGES

Norris J. Huffington, Jr.
William O. Ewing

September 1985

US ARMY BALLISTIC RESEARCH LABORATORY
ABERDEEN PROVING GROUND, MARYLAND

Destroy this report when it is no longer needed.
Do not return it to the originator.

Additional copies of this report may be obtained from the National Technical Information Service, U. S. Department of Commerce, Springfield, Virginia 22161.

The findings in this report are not to be construed as an official Department of the Army position, unless so designated by other authorized documents.

The use of trade names or manufacturers' names in this report does not constitute indorsement of any commercial product.

UNCLASSIFIED

SECURITY CLASSIFICATION OF THIS PAGE *(When Data Entered)*

REPORT DOCUMENTATION PAGE		READ INSTRUCTIONS BEFORE COMPLETING FORM
1. REPORT NUMBER TECHNICAL REPORT BRL-TR-2678	2. GOVT ACCESSION NO. AD-A160797	3. RECIPIENT'S CATALOG NUMBER
4. TITLE *(and Subtitle)* Reflected Impulse Near Spherical Charges		5. TYPE OF REPORT & PERIOD COVERED Final 6. PERFORMING ORG. REPORT NUMBER
7. AUTHOR(s) Norris J. Huffington, Jr. William C. Ewing		8. CONTRACT OR GRANT NUMBER(s)
9. PERFORMING ORGANIZATION NAME AND ADDRESS USA Ballistic Research Laboratory ATTN: AMXBR-VLD Aberdeen Proving Ground, MD 21005-5066		10. PROGRAM ELEMENT, PROJECT, TASK AREA & WORK UNIT NUMBERS 1L161102AH43
11. CONTROLLING OFFICE NAME AND ADDRESS USA Ballistic Research Laboratory ATTN: AMXBR-OD-ST Aberdeen Proving Ground, MD 21005-5066		12. REPORT DATE September 1985 13. NUMBER OF PAGES 64
14. MONITORING AGENCY NAME & ADDRESS *(if different from Controlling Office)*		15. SECURITY CLASS. *(of this report)* UNCLASSIFIED 15a. DECLASSIFICATION/DOWNGRADING SCHEDULE

16. DISTRIBUTION STATEMENT *(of this Report)*

Approved for public release; distribution unlimited.

17. DISTRIBUTION STATEMENT *(of the abstract entered in Block 20, if different from Report)*

18. SUPPLEMENTARY NOTES

19. KEY WORDS *(Continue on reverse side if necessary and identify by block number)*

Air Blast,	Reflected Pressure,	Scaling Laws,
Shock Waves,	Reflected Impulse,	Regular Reflection,
Spherical Charges,	Hydrocode	Mach Reflection,
Pentolite Explosive,	Plug Experiments,	Pulse Duration.

20. ABSTRACT *(Continue on reverse side if necessary and identify by block number)*

Experiments were performed at small scaled distances using the impulse plug technique in an effort to resolve discrepancies between empirical data for reflected impulse and results derived using the HULL hydrocode. Scaled normally reflected impulse data are provided for scaled distances in the range 0.06 to 0.20 m/kg$^{1/3}$ (0.15 to 0.50 ft/lb$^{1/3}$). Keywords: (cont. kg) (cont. lb.)

DD FORM 1473 EDITION OF 1 NOV 65 IS OBSOLETE

UNCLASSIFIED

SECURITY CLASSIFICATION OF THIS PAGE *(When Data Entered)*

TABLE OF CONTENTS

LIST OF ILLUSTRATIONS

I. INTRODUCTION

The requirement for rational analytic procedures to predict damage to lightly armored vehicles and aircraft caused by high explosive warhead detonations in close proximity to such targets provided the motivation for the investigation to be reported. It would obviously simplify the development of such procedures if the loading produced by the warhead could be predicted independently from the structural response analysis. While this uncoupling cannot be justified in general, the extremely short duration of the positive phase of blast pulses from small explosive charges in comparison to the time for appreciable response of moderately hard targets suggests that this simplification may be suitable for the contemplated application. However, it must be recognized that even when the blast pulse approaches a pure impulse, the relative delivery times of such pulses at different portions of the structure must be adequately represented.

While it is recognized that fragments from detonating warheads are effective in producing target damage and interact synergistically with airblast effects on targets, it was preferred to start this investigation by attempting to define the load distribution produced by bare charges since it was this augmenting damage mechanism which had not been taken into account in earlier vulnerability models. Also, there is interest in the effects of lightly cased munitions for which the contribution of fragments to the total loading is insignificant. Consequently, attention was directed to the idealized problem of defining the blast loading on a large flat surface produced by center-initiated bare spherical charges at various stand-offs. It had been expected that it would be possible to produce an empirically-based computer program which would provide the blast pressure-time history for given input parameters. In fact, Mr. K. O. Opalka has developed such a program, but its release has been deferred owing to doubts regarding its data base for the region around the transition from regular to Mach reflection and for small scaled heights-of-burst.* The existing data gaps and contradictions will be discussed in the next section.

It will be seen that prediction of normally reflected pressure and impulse for small Z is clouded in considerable uncertainty, i.e., there are large differences between scaled experimental data and a corresponding hydrocode prediction. This prompted an effort to obtain blast data for the cited small Z range. However, the present status of pressure transducers appeared to preclude measurements in this very high pressure region. On

---

* Hopkinson[1] scaled distances Z less than 0.2 $m/kg^{1/3}$ (0.5 $ft/lb^{1/3}$).

[1] B. Hopkinson, British Ordnance Board Minutes 13565,1915.

the other hand, it seemed entirely feasible to employ a previously used impulse plug technique[2] to obtain data for reflected impulse. Such experiments were performed and the resulting information and comparisons with other sources are given in the sequel.

II. REVIEW OF EXISTING INFORMATION

An examination of the widely referenced compilation of blast data by Goodman[3] reveals that none of these data involved actual pressure or impulse measurements for $Z < 0.2$ m/kg$^{1/3}$ (0.5 ft/lb$^{1/3}$). Certain information on normally reflected impulse for smaller Z is listed but reference to the source[4] reveals that this information was based on Sachs' scaling[5] of data obtained in a reduced pressure environment and no shots were fired closer than the Z cited above. Subsequent data from tests at BRL appear to have the same limitation.

Some closer range pressure and impulse data have been reported[6] by Southwest Research Institute personnel. These data provided information on reflected peak pressure and reflected impulse at various radial distances from "ground zero" along a flat surface. The closest reported scaled distance was 0.12 m/kg$^{1/3}$ (0.3ft/lb$^{1/3}$).

Another source of information for reflected pressures is the report by Kingery and Pannill,[7] which is based on the theoretical treatment of regular reflection by J. von Neumann.[8] This report provides tables of incident and reflected overpressure, dynamic

---

[2] O. T. Johnson, J. D. Patterson II, and W. C. Olson, "A Simple Mechanical Method for Measuring the Reflected Impulse of Air Blast Waves," Ballistic Research Laboratories Memorandum Report No. 1088, July 1957.

[3] H. J. Goodman, "Compiled Free-Air Blast Data on Bare Spherical Pentolite," Ballistic Research Laboratories Report No. 1092, February 1960.

[4] W. C. Olson, J. D. Patterson II, and J. S. Williams, "The Effect of Atmospheric Pressure on the Reflected Impulse from Air Blast Waves," Ballistic Research Laboratories Memorandum Report No. 1241, January 1960.

[5] R. G. Sachs, "The Dependence of Blast on Ambient Pressure and Temperature," Ballistic Research Laboratory Report No. 466, May 1944.

[6] J. J. Kulesz, E. D. Esparza, and A. B. Wenzel, "Blast Measurements at Close Standoff Distances for Various Explosive Geometries," Minutes of the Eighteenth Explosives Safety Seminar, Vol. I, pp. 405-445, September 1978.

[7] C. N. Kingery and B. F. Pannill, "Parametric Analysis of the Regular Reflection of Air Blast," Ballistic Research Laboratories Report No. 1249, June 1964.

[8] R. Courant and K. O. Friedrichs, "Supersonic Flow and Shock Waves," Interscience Publishers, New York, 1948, pp. 327-331.

pressure and angles of the incident and reflected shocks as a function of horizontal distance for selected scaled heights-of-burst. These values were computed using the von Neumann model and data for γ (ratio of specific heats) for air as a function of overpressure. The model does not take account of explosion products so the results may not be representative of an actual explosion.

The writer felt it would be useful to make predictions of reflected pressure and impulse for a small Z appropriate for a warhead detonation, employing all available sources and extrapolations from these. The case of blast from a 0.907 kg (2 pound) 50/50 Pentolite charge detonated with its center at height H of 63.5 mm (2.5inches) above an infinite rigid plane was chosen for comparisons.

At the writer's request Mr. R. E. Lottero employed the HULL[9] hydrocode to obtain a numerical solution for this case. The results of his calculations are compared with predictions based on the previously cited sources (or extrapolations therefrom) in the following figures. Figure 1 shows the peak reflected pressure on the plane surface as a function of the radial distance along the plane from "ground zero." The corresponding reflected impulse distribution is represented in Figure 2. The most significant results of these comparisons is that the peak normally reflected pressure predicted by the hydrocode is greater than any of the empirically derived values while for the normally reflected impulse the converse is true, the differences being as much as a factor of two. The figures also show that these discrepancies exist not only directly under the charge but also over much of the range of R/H where the pressures and impulses are large. Consequently, until these discrepancies can be resolved, structural response predictions based on such distributions are also subject to serious doubts.

Before arriving at conclusions regarding the significance of the variance between the curves in Figures 1 and 2, it is appropriate to take a critical look at the basis for each of these. Also, there are three fluid dynamic regimes to consider:

(1) The region of regular shock reflection which applies until the angle at which the incident shock strikes the plane reaches a critical value, for this case corresponding to R/H $\approx$ 0.9.

(2) The region of irregular Mach reflection which features a two triple point shock structure. The upper limit on R/H for this region is not known for this case but is reached when the two triple points coalesce.

(3) Beyond the irregular Mach region there is the regular Mach reflection zone which applies for all greater values of R/H.

---

[9] D. A. Matuska and R. E. Durrett, "The HULL Code, A Finite Difference Solution to the Equations of Continuum Mechanics," AFATL-TR-78-125, November 1978.

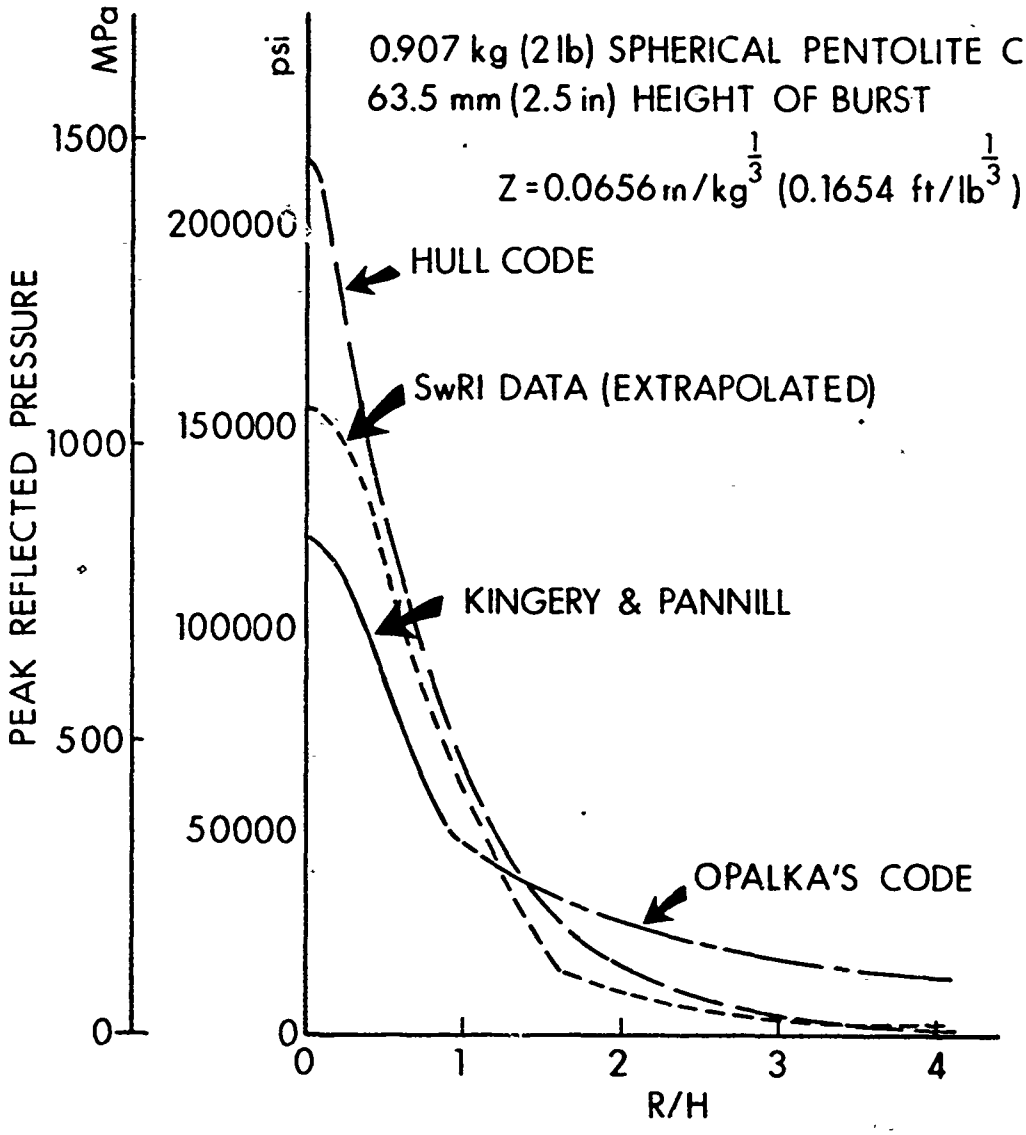

Figure 1. Spatial Distribution of Peak Reflected Pressure

The curve in Figure 1 labeled Kingery and Pannill was obtained by interpolation of their tables, which are based on von Neumann's theory for the regular reflection regime. These tables apply to shocks in air, with the ratio of specific heats γ treated as a function of incident overpressure. Since, for small Z, the explosion products reach the plane surface it is believed that the reflected overpressures are actually somewhat greater. The von Neumann model does not consider the tail of the blast wave so no information on reflected impulse can be derived thereby.

The curves representing extrapolations of Southwest Research Institute data were provided by Mr. C. Kingery. While these extrapolations were carefully performed, the writer has determined through examination of the scatter in the original data and taking account of the fact that the "nearest" experimental data are for

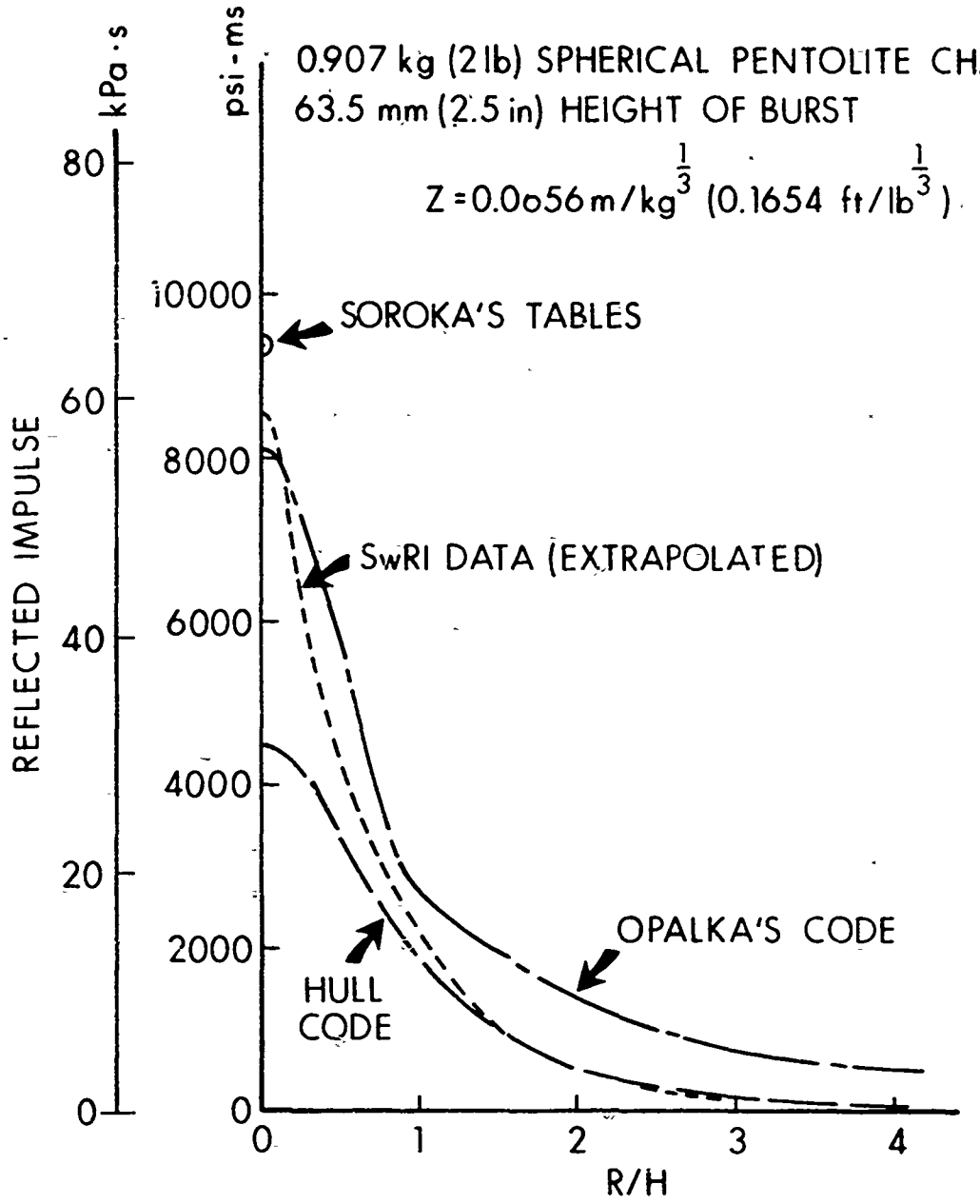

Figure 2. Spatial Distribution of Reflected Impulse

$Z = 0.12 m/kg^{1/3}$ $(0.3 ft/lb^{1/3})$ that a broad band centered on these curves would be more appropriate.

The single data point on Figure 2 at $R/H = 0$ was obtained by interpolation using Table B of a report by Soroka.[10] However, the data source for this portion of the table

---

[10] B. Soroka, "Air Blast Tables for Spherical 50/50 Pentolite Charges at Side-On and Normal Incidence," Ballistic Research Laboratory Memorandum Report ARBRL-MR 02975, December 1979.

is the previously cited report by Olson, Patterson, and Williams[4] concerned with impulse plug experiments performed in an evacuated chamber. The authors of this report were rightly concerned about a possible misinterpretation of their data, for if sea level atmospheric pressure is substituted in Sachs' scaling parameter one might infer that their data included a firing where the height-of-burst was less than the radius of the explosive charge!

For large values of R/H (i.e., well into the regular Mach reflection regime) the HULL code predictions and the extrapolated Southwest Research Institute data tend to coalesce. This should occur because at these ranges accurate experimental measurements of pressures can be made with piezoelectric transducers and because hydrocode solutions become insensitive to the modeling of the initiation process. More significantly, these predictions appear to asymptotically approach values associated with the limiting situation depicted in Figure 3. In Figure 3(a) the shock structure above an ideal reflecting plane for the regular Mach reflection region is shown for a spherical charge of weight W at a low height-of-burst H. Obviously the same shock structure would occur if the reflecting plane were removed and a second charge of weight W and height-of-burst -H was detonated simultaneously. At sufficiently large values of R the blast parameters for the case (Figure 3(a)) shown become the same as those for the case shown in Figure 3(b); i.e., for a free field burst of charge weight 2W at the point 0. This suggests that, for large R/H, the blast loading on the panel surface can be constructed using tabulated side-on blast parameters for a doubled charge weight.

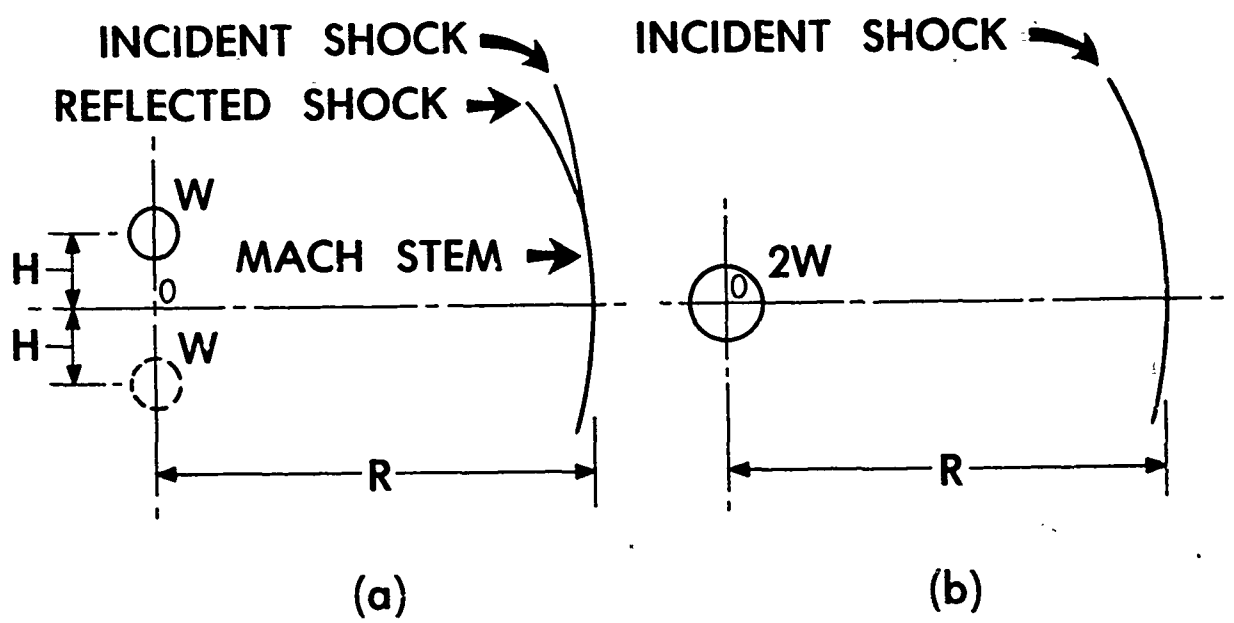

Figure 3. Equivalent Air Blasts at Large R

Mr. Opalka's code attempted to combine various empirical models to provide load predictions for the three shock reflection regimes previously cited. For the regular reflection region his code employed the von Newmann model for peak reflected pressures and, using the same spatial distribution, determined impulses to match tabulated data for reflected normally impulse (which assumed the Sachs' scaling law). For the Mach region the code employed an adaptation of an empirical model due to Moore,[11] which was not derived for blast from spherical charges and which seems to overpredict the loading for large R/H.

In summary, the writer found no experimental data which were obtained for the small scaled distance range of interest. Extrapolation from data for larger scaled distances or acceptance of Sachs' scaling lead to large differences from hydrocode predictions in both peak reflected pressure and reflected impulse. The modest test program presented in the next section was undertaken for the purpose of resolving at least some of these discrepancies.

III. THE EXPERIMENTAL PROGRAM

A. Test Facility

Since pressure transducers are not available which can survive and function in the very high pressure region directly under the charge (cf, Figure 1) it was decided to employ the impulse plug technique in a similar manner to that reported by Johnson, Patterson and Olson.[2] To avoid problems with plugs binding in holes the method was used only to measure normally reflected impulse. The analysis employed to interpret the test data will be presented later in this report. The facility which had been built for the previous tests was still available and was modified for use in this series (see Figure 4). This facility was basically a cubicle with a roof of 25.4 mm (1 inch) thick armor plate containing a cylindrical hole through which the plug was projected by the explosive blast. Some preliminary firings were performed for $Z = 0.2$ m/kg$^{1/3}$ (0.5 ft/lb$^{1/3}$) in the original facility but it was realized that the roof would be inadequate for smaller scaled distances so most of the roof was replaced by a slab of 76.2 mm (3 inch) rolled homogeneous steel armor plate. This slab was of sufficient size that the effects of shock diffraction at the edge would not have time to propagate back to the plug during the positive phase of the air blast.

Both Figures 4 and 5 show the metal frame used to support the explosive charge. In figure 5 an explosive charge has been taped to a cardboard tube which is affixed to the vertical adjustment rod of the support frame. Since the standoff becomes very critical for small Z a special adjustable feeler gage was developed to control the gap between the plug and the surface of the spherical charge.

---

[11] G. R. Moore, "Calculations of the Reflected Overpressure and Transient Loading on a Deck from Elevated Gun Fire," Naval Weapons Laboratory Technical Report TR-2847, November 1972.

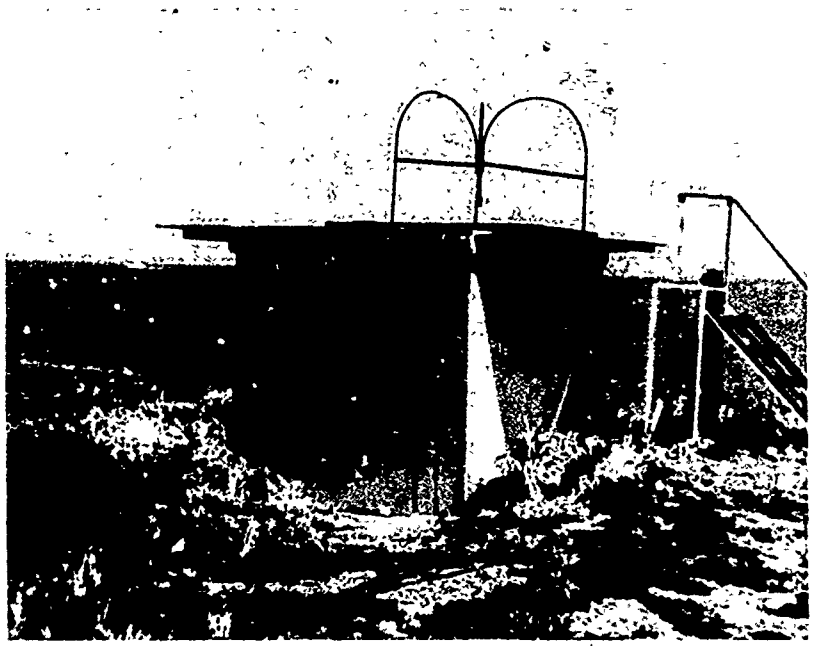

Figure 4. Impulse Plug Test Facility

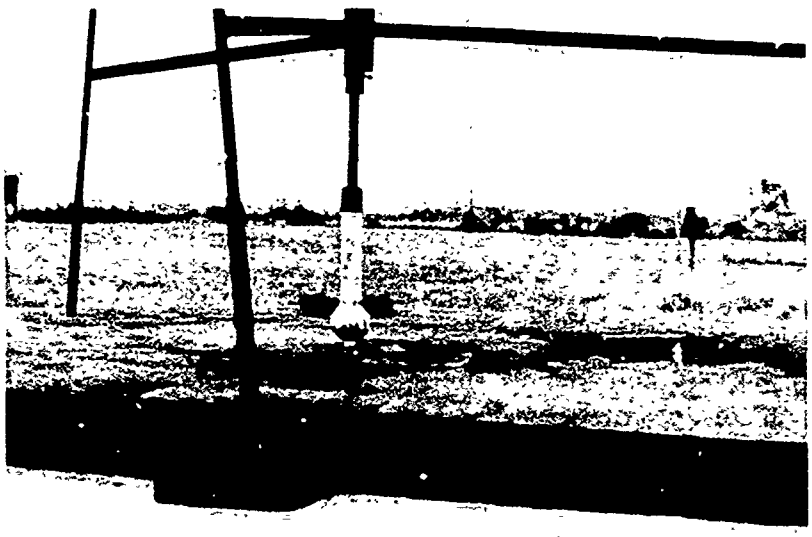

Figure 5. Spherical Charge Supported Above Armor Plate

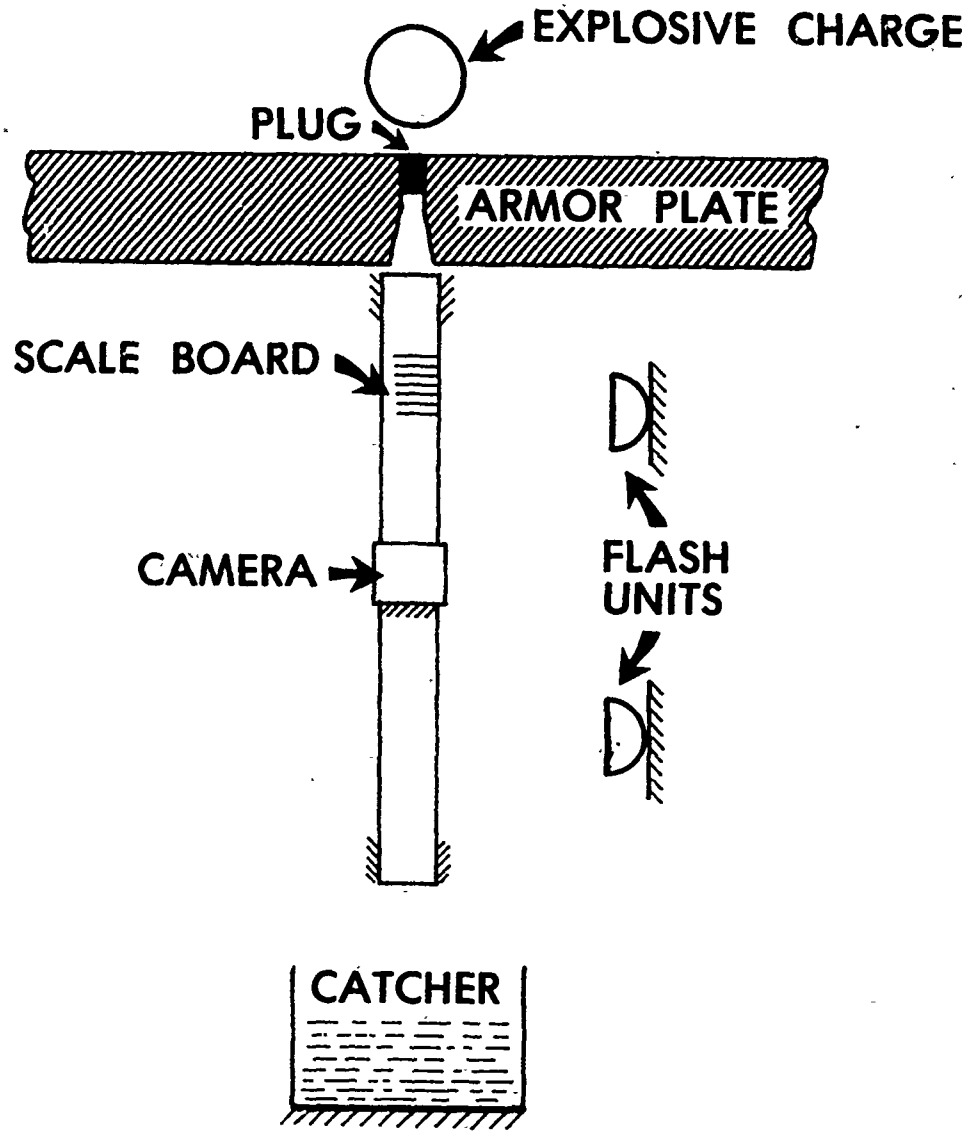

Figure 6. Schematic Section Through Test Facility

Figure 6 is a schematic drawing of the interior of the cubicle. A nominal 12.7 mm (0.500 inch) diameter hole was bored through the roof, then a 15° conical reamer was used as indicated to minimize interference with the plug during projection. The plugs were recovered in a box on the floor of the cubicle which was filled with celotex and plywood.

B. Instrumentation

It was preferred to determine the plug velocity by purely optical means. Accordingly, a vertical scale was mounted on a board closely paralleling the expected path of the plug. Two capacitance discharge (spark gap) flash units were positioned as

indicated in Figure 6 and a Polaroid camera with a Wollensack 162 mm/F4.5 lens was mounted so as to view the plug passing in front of the scale. During a test the cubicle is darkened and an automatic sequencer opens the camera shutter as the firing begins, causes each flash unit to function as the plug is at about its level and then closes the camera shutter. The precise time of each flash is recorded on a Nicolet digital oscilloscope. Since the flash durations are sufficiently short to "stop" the plug motion the corresponding positions of the plug can be read from the Polaroid print which include the vertical scale.

C. The Impulse Plugs

The following cons. erations were taken into account in the design of the plug specimens:

1. The pressure distribution on the top of the plug should be as uniform as possible; this dictated reducing the diameter of the plug to about 12.7 mm (0.500 inch) diameter due to the close proximity of the spherical charge.
2. The clearance between plug and hole should be minimized to avoid diffractive unloading of the top surface of the plug and blow-by of explosion products, yet be sufficient that Poisson-type deformation of plate and plug under stress should not produce frictional resistance to motion of the plug. As a compromise the following machining dimensions were selected:

   Plug diameter $12.45^{+.000}_{-.025}$ mm $(0.490^{+.000}_{-.001}$ in)

   Hole diameter $12.70^{+.025}_{-.000}$ mm $(0.500^{+.001}_{-.000}$ in)

   For elastic deformation including dynamic overshoot these tolerances should provide 0.127 mm (0.005 in) clearance for a concentrically positioned plug.
3. The plug should remain intact and not experience signifi-ant plastic deformation when subjected to longitudinal stress waves resulting from blast loading. Initially, rolled homogeneous armor was selected as the plug material on the basis of its toughness. These plugs performed satisfactorily for the larger scaled distances in this series but as Z was reduced it was observed that appreciable radial plastic deformation occurred near the loaded end. Following this, plugs were machined from Bearcat tool steel which has a higher yield strength. No problems with either plastic deformation or fracture were experienced with the latter specimens.
4. The plug should acquire a velocity within a range of values which can be determined with sufficient accuracy by the available apparatus. The plug velocity depends upon the blast impulse and its mass. The latter can be controlled by varying the length of the plug; it was found that use of 25.4 mm (1 inch) long plugs produced satisfactory velocities for the entire range of scaled distances tested.

D. Plug Response Analysis

The analysis required for interpretation of the test data is considered in detail in Appendix A. By definition the impulse delivered to the plug (actually, impulse per unit area) is:

$$I = \int_o^T p(t)\,dt \qquad (1)^*$$

This impulse can be evaluated for individual test data sets by use of

$$I = \frac{m}{A}\sqrt{\left\{\frac{x_2 - x_1}{t_2 - t_1} - \frac{g}{2}(t_2 - t_1)\right\}^2 - 2gx_1} \qquad (2)$$

provided that the following assumptions are satisfied for the particular test;

1. The displacement of the plug during the blast pulse must be very small. This assumption can be evaluated for specific tests by using the formulation given in Appendix A with plausible values of the pulse duration.
2. Friction between plug and plate are negligible. This is necessary to obtain satisfactory values for the impulse; data for tests where binding was suspected were discarded.
3. Air drag forces are negligible. This was presumed to be true because the velocities of the plugs were not high enough to induce significant drag forces and because, for a considerable portion of its motion, the plug was surrounded by explosion products moving at a higher velocity.

The formulation represented by Equation (2) is identical with that employed by Johnson, Patterson, and Olson.[2]

---

* Symbols are defined in the List of Symbols, page 37.

E. Experimental Design

In order to obtain sufficient data to map out the variation of normally reflected impulse versus scaled distance it was decided to perform tests at the following values of Z:

Z	
$m/kg^{1/3}$	$ft/lb^{1/3}$
0.198	0.5
0.159	0.4
0.119	0.3
0.079	0.2
0.066	0.1654*
0.060	0.15

If these were all successful it is likely that an attempt would have been made to measure I until the surface of the charge was reached; i.e., to $Z = 0.0525\ m/kg^{1/3}$ ($0.1323\ ft/lb^{1/3}$).

Also, since it was not established that the Hopkinson scaling law applies for such small Z, it was desired to obtain data for more than one charge weight; specifically for charges of 0.227, 0.454, 0.907 kg (0.5, 1.0, 2.0 lb).

From examination of standard deviations from earlier tests it was concluded that three tests at each parameter-pair would yield results at the 95% confidence level while the 99% level could be reached for five replications.

F. Testing Experience

The tests were conducted primarily in order of decreasing scaled distance. Figure 7 shows a representative photograph of the vertical scale with the plug "stopped" at two positions by the flash lamps. Because the lamps are to the right of the camera the shadow of the plug is to the left of the plug. In order to reduce the data one must estimate the vertical positions of the mass center; i.e., x_1 and x_2 of Equation (2). This is made somewhat more difficult by the fact that, in spite of care in centering the plug and the explosive charge, most of the plugs experienced some tumbling. This tumbling does not invalidate the response formulation but could increase the drag force. In a few instances the tumbling plug hit the scale; if this occurred above x_2 the results of that test were discarded.

---

* This value was chosen to correspond to the case discussed in Section II.

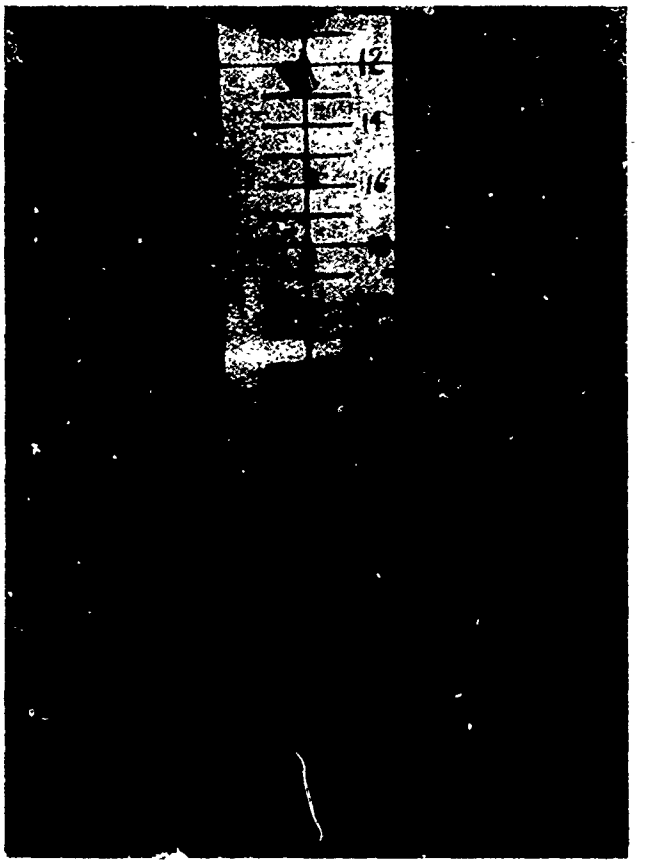

Figure 7. Dual Image of Plug in Front of Scale

For the series of tests with 0.079 kg (2.0 lbs) charges at $Z = 0.079$ m/kg$^{1/3}$ (0.[illegible] ft/lb$^{1/3}$) the RHA plugs were significantly deformed so that it was necessary to use the hardened BEARCAT plugs. The RHA armor plate also experienced plastic flow and cratering, the latter increasing in size and depth as the tests continued at smaller Z. It was found necessary to ream out the cylindrical hole in the plate to its original diameter before each shot. Another problem arose concerning the photographs of the plug against the scale background: fiery streaks (burning explosive or metal) either blowing by or following the plug obscured the image of the plug resulting in loss of data. Efforts to prevent this by use of baffles were not very successful.

For the smaller scaled distances there was concern that the plastic flow of the plate (decrease of hole diameter) during the blast response might result in resistance to plug ejection. Accordingly, the cylindrical surface of the plugs was given a thin coating of manganese disulfide powder in the belief that its lubrication property would help circumvent this possibility.

When the depth and extent of the crater in the armor plate became significant a few shots were fired in which the crater was filled with "epoxy steel." This served to restore the original plate/plug geometry at the initiation of the shot. However, this material was all removed by the blast and it was feared that some of this material might intrude into the gap between plug and plate. At the end of this test program while attempting to obtain data for 0.227kg (0.5 lb) charges at $Z = 0.060$ m/kg$^{1/3}$ (0.15 ft/lb$^{1/3}$), two shots were fired in which hardened steel inserts were pressed into holes counterbored to a depth of 22.2 mm (0.875 in)in the armor plate. These inserts were also flush with the original plate surface and the crater outside the inserts was filled with the epoxy material. A more positive retention method would be required for further testing since the inserts were ejected during the rebound phase of the plate response.

G. Impulse Data

The basic data obtained from the impulse plug tests are tabulated in Appendix B. From these data the values of the Hopkinson scaling parameters Z and $I/W^{1/3}$ were calculated and are presented in Table 1, grouped by the nominal value of Z and, for each of these, by the nominal charge weight. Out of the fifty-seven tests for which complete data were obtained, two were regarded with suspicion and their results were rejected on the basis of several criteria for treatment of outliers.[12] These tests are indicated by asterisks in Table 1 and their results were not used in the calculations of mean impulses or standard deviations.

The validity of the Hopkinson scaling law was then investigated using the statistical technique of analysis of variance. The F-statistic was employed at the 95% confidence level to test the hypothesis that all the scaled impulses for each nominal scaled distance were derived from the same normal population. According to this procedure one would conclude that this hypothesis is valid for $Z \geq 0.159$ m/kg$^{1/3}$ (0.4 ft/lb$^{1/3}$) but should be rejected for all smaller Z for which data are available. Thus, it appears that the Hopkinson scaling law becomes questionable as the charge approaches the reflecting surface. Such a deduction is certainly subject to challenge, however. The charge weights have been varied over only a small range and the standard deviations σ of the scaled impulses increase as Z decreases. It is unfortunate that the range of Z for which a larger data sample is required is just the one where the tests are most difficult to perform. On the other hand it is noted that for $Z < 0.159$ m/kg$^{1/3}$ (0.4 ft/lb$^{1/3}$), the values of $I/W^{1/3}$ at each Z exhibit a monotone decrease as charge weight increases.

The values of mean scaled impulse $\overline{(I/W^{1/3})}$ are plotted against Z in Figure 8, using a different symbol for each charge weight. Where they do not conflict with other symbols " $\pm 3\sigma$ bars" have been added to data points for the 0.227 kg (0.5 lb) charges.

---

[12] M. G. Natrella, Engineering Design Handbook, Experimental Statistics, Section 4, Chapter 17, AMCP 706-113, March 1966.

TABLE 1. SCALED TEST RESULTS

$Z_{nominal} = 0.2\ (0.5)^*$		
Test No.	Z	$I/W^{1/3*}$
0.454 kg (1 lb) Pentolite (approximately)		
33	.1990 (.5017)	7.22 (804.)
34	.1985 (.5004)	7.32 (816.)
35	.1980 (.4992)	7.29 (813.)
36	.1979 (.4989)	7.22 (804.)
37	.1976 (.4982)	7.19 (801.)
$\bar{Z} = 0.1982\ (0.4997)$ $\quad \sigma_Z = 0.0006\ (0.0014)$ $\overline{I/W^{1/3}} = 7.248\ (807.7)$ $\quad \sigma = 0.057\ (6.4)$		
0.907kg (2 lb) Pentolite (approximately)		
65	.1982 (.4997)	7.17 (799.)
66	.1981 (.4995)	7.07 (788.)
67	.1980 (.4992)	7.29 (813.)
68	.1989 (.5013)	7.37 (821.)
69	.1982 (.4997)	6.94 (773.)
$\bar{Z} = 0.1983\ (0.4999)$ $\quad \sigma_Z = 0.0003\ (0.0008)$ $\overline{I/W^{1/3}} = 7.168\ (798.8)$ $\quad \sigma_I = 0.171\ (19.1)$		

*Units:

Z, σ_Z $\quad m/kg^{1/3}\ (ft/lb^{1/3})$

$I/W^{1/3}, \sigma_I$ $\quad kPa{\cdot}s/kg^{1/3}\ (psi{\cdot}ms/lb^{1/3})$

TABLE 1. SCALED TEST RESULTS (CONT'D)

$Z_{nominal} = 0.16\ (0.4)$		
Test No.	Z	$I/W^{1/3}$
0.227 kg (0.5 lb) Pentolite (approximately)		
98	.1612 (.4065)	10.71 (1194.)
99	.1588 (.4003)	10.73 (1196.)
100	.1588 (.4002)	10.98 (1224.)
101	.1585 (.3996)	10.86 (1210.)
102	.1585 (.3995)	10.72 (1194.)
$\overline{Z} = 0.1592\ (.4012)$		$\sigma_Z = 0.0012\ (0.0030)$
$\overline{I/W^{1/3}} = 10.800\ (1203.6)$		$\sigma_I = 0.119\ (13.3)$
0.454 kg (1.0 lb) Pentolite (approximately)		
38	.1590 (.4007)	11.03 (1229.)
39	.1588 (.4004)	10.83 (1207.)
40	.1588 (.4003)	10.91 (1216.)
41	.1585 (.3995)	10.90 (1215.)
42	.1583 (.3989)	10.95 (1220.)
$\overline{Z} = 0.1587\ (0.4000)$		$\sigma_Z = 0.0003\ (0.0007)$
$\overline{I/W^{1/3}} = 10.925\ (1217.5)$		$\sigma_I = 0.074\ (8.3)$
0.907 kg (2 lb) Pentolite (approximately)		
70	.1588 (.4004)	11.03 (1229.)
71	.1587 (.4001)	10.71 (1193.)
72	.1586 (.3998)	10.86 (1211.)
74	.1603 (.4041)	10.10 (1126.)*
75	.1589 (.4005)	10.86 (1211.)
$\overline{Z} = 0.1588\ (0.4002)$		$\sigma_Z = 0.0001\ (0.0003)$
$\overline{I/W^{1/3}} = 10.865\ (1210.8)$		$\sigma_I = 0.130\ (14.5)$

TABLE 1. SCALED TEST RESULTS (CONT'D)

$Z_{nominal} = 0.12$ (0.3)		
Test No.	Z	$I/W^{1/3}$
0.227 kg (0.5 lb) Pentolite (approximately)		
103	.1209 (.3048)	19.74 (2200.)
104	.1192 (.3006)	19.97 (2226.)
107	.1183 (.2983)	19.82 (2208.)
109	.1187 (.2992)	19.54 (2178.)
110	.1186 (.2989)	19.12 (2131.)
$\bar{Z} = 0.1191$ (0.3003) $\quad \sigma_Z = 0.0010$ (0.0026) $\overline{I/W^{1/3}} = 19.640$ (2188.6) $\quad \sigma_I = 0.329$ (36.6)		
0.454 kg (1.0 lb) Pentolite (approximately)		
43	.1196 (.3015)	18.86 (2101.)
44	.1196 (.3014)	18.40 (2050.)
45	.1192 (.3005)	18.51 (2063.)
52	.1190 (.3000)	17.35 (1934.)*
54	.1195 (.3012)	18.92 (2109.)
56	.1192 (.3005)	19.04 (2122.)
$\bar{Z} = 0.1194$ (0.3010) $\quad \sigma_Z = 0.0092$ (0.0005) $\overline{I/W^{1/3}} = 18.745$ (2089.0) $\quad \sigma_I = 0.276$ (30.8)		
0.907 kg (2.0 lb) Pentolite (approximately)		
76	.1200 (.3026)	18.04 (2011.)
77	.1194 (.3009)	18.94 (2110.)
78	.1190 (.3001)	18.78 (2092.)
79	.1190 (.2999)	18.78 (2093.)
80	.1189 (.2997)	18.83 (2098.)
$\bar{Z} = 0.1193$ (0.3006) $\quad \sigma_Z = 0.0005$ (0.0012) $\overline{I/W^{1/3}} = 18.673$ (2080.9) $\quad \sigma_I = 0.358$ (39.8)		

TABLE 1. SCALED TEST RESULTS (CONT'D)

$Z_{nominal} = 0.08\ (0.2)$		
Test No.	Z	$I/W^{1/3}$
0.227 kg (0.5 lb) Pentolite (approximately)		
111	.0790 (.1992)	41.9 (4670.)
112	.0790 (.1991)	41.8 (4660.)
113	.0794 (.2003)	45.2 (5040.)
114	.0794 (.2001)	43.6 (4860.)
115	.0794 (.2001)	45.7 (5090.)
$\overline{Z} = 0.0792\ (0.1997)$ $\quad \sigma_Z = 0.0002\ (0.0006)$ $\overline{I/W^{1/3}} = 43.65\ (4865.) \quad \sigma_I = 1.81\ (202.)$		
0.454 kg (1.0 lb) Pentolite (approximately)		
92	.0796 (.2006)	41.0 (4570.)
93	.0795 (.2003)	42.3 (4710.)
95	.0793 (.1999)	42.6 (4740.)
96	.0799 (.2014)	42.2 (4710.)
97	.0796 (.2008)	43.2 (4810.)
$\overline{Z} = 0.0796\ (0.2006) \quad \sigma_Z = 0.0002\ (0.0006)$ $\overline{I/W^{1/3}} = 42.26\ (4709.) \quad \sigma_I = 0.78\ (86.5)$		
0.907 kg (2.0 lb) Pentolite (approximately)		
83	.0794 (.2001)	40.4 (4500.)
84	.0793 (.1999)	40.3 (4500.)
87	.0793 (.1998)	39.0 (4340.)
$\overline{Z} = 0.0793\ (0.1999) \quad \sigma_Z = 0.0006\ (0.0002)$ $\overline{I/W^{1/3}} = 39.90\ (4446.) \quad \sigma_I = 0.80\ (89.0)$		

TABLE 1. SCALED TEST RESULTS (CONT'D)

Test No.	Z	$I/W^{1/3}$
0.907 kg (2.0 lb) Pentolite (approximately)		
89	.0656 (.1653)	53.227 (5930.)

$Z_{nominal} = 0.08$ (0.15)		
0.227 kg (0.5 lb) Pentolite (approximately)		
116	.0595 (.1501)	70.8 (7890.)
125	.0592 (.1493)	67.9 (7570.)
$\bar{Z} = 0.0594$ (0.1497)	$\sigma_Z = 0.0002$ (0.0005)	
$\overline{I/W^{1/3}} = 69.36$ (7729.)	$\sigma_I = 2.01$ (224.)	

Curves have been drawn through the data points for the smallest and largest charges tested. These curves are seen to coalesce for the Z range where the Hopkinson law was validated by the statistical analysis and to fair in nicely with the data of Johnson, Patterson, and Olson[2] for larger Z.

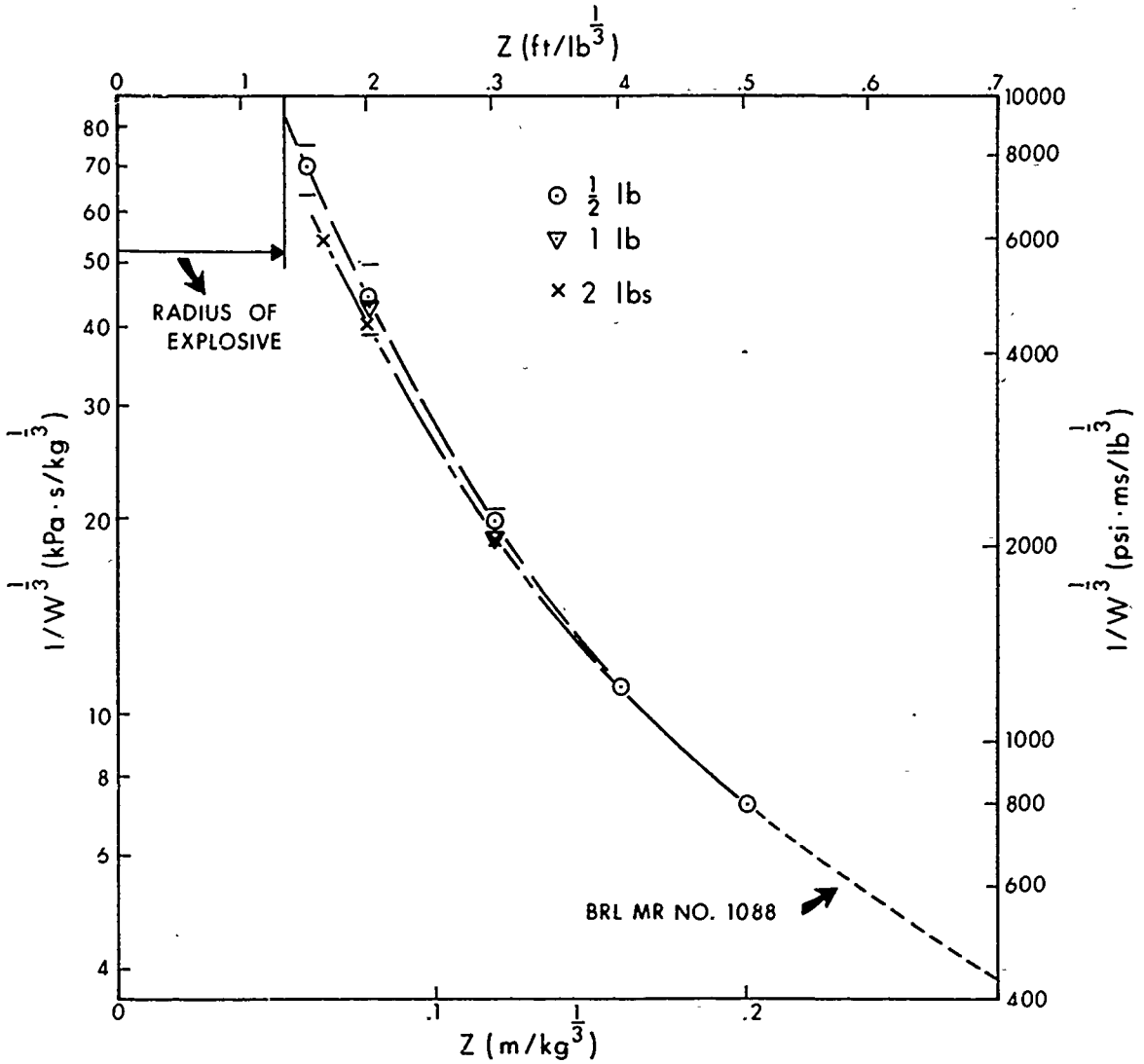

Figure 8. Scaled Impulse Versus Scaled Distance

One could certainly draw a single "best-fit" curve for all the data of this report; however, this could be misleading if significantly different charge weights were to be used. While the cause of this apparent dependence of scaled impulse on charge weight for small Z has not been identified it should be noted that geometric scaling was not preserved in these experiments in that no attempt was made to vary the diameter of the plug as Z was varied. Figure 9 compares the geometries of the charge/plug configurations at the extremes of charge weights and smallest Z tested.

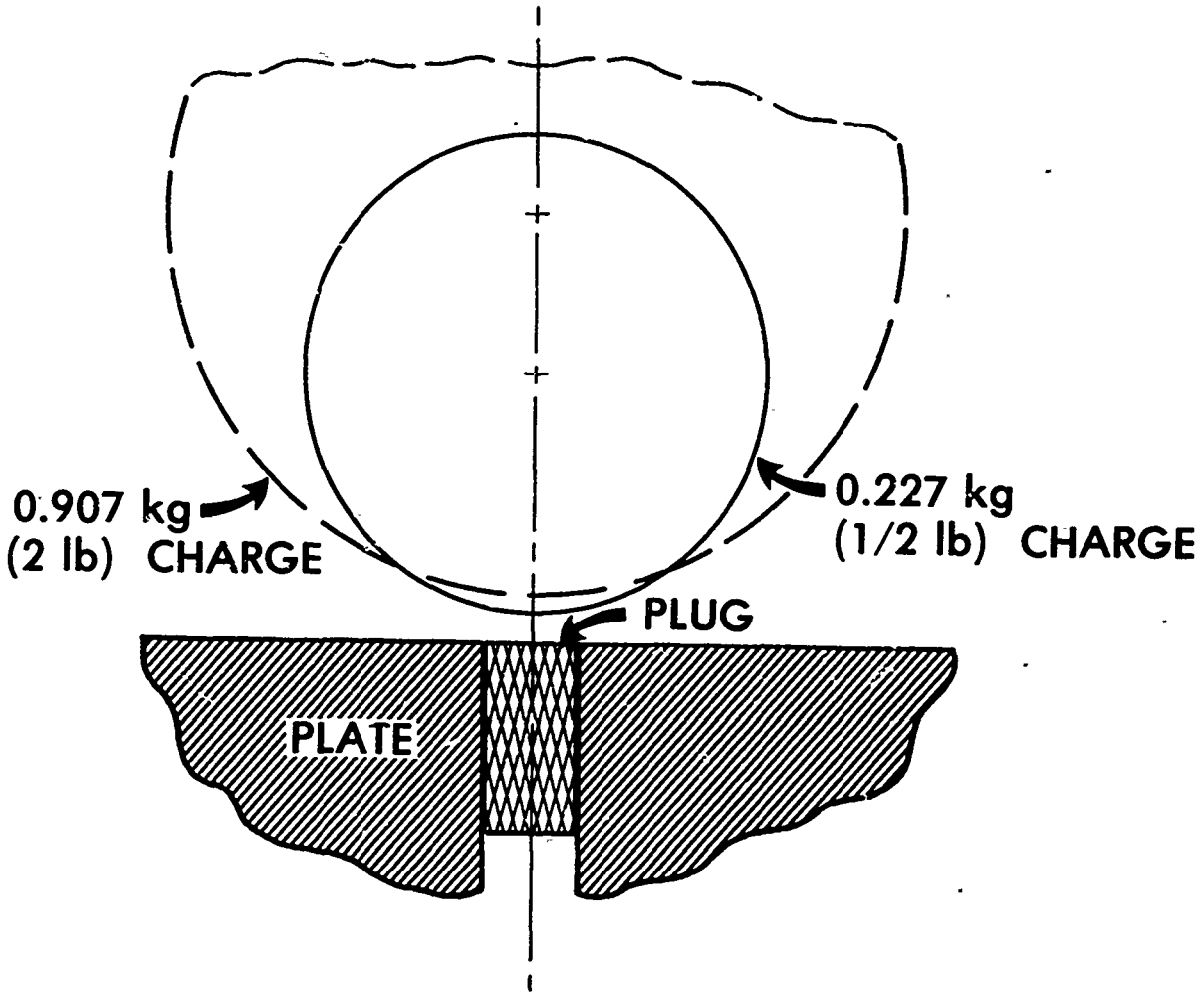

Figure 9. Comparison of Geometries at $Z = 0.060$ m/kg$^{1/3}$ (0.15 ft/lb$^{1/3}$)

H. Pressure Measurements

During this investigation three exploratory tests were performed in which reflected overpressures were recorded. Two PCB Model No. 109A piezoelectric transducers were mounted flush with the upper surface of the armor plate and 152.4 mm (6 in) apart. The spherical charge was positioned directly above one of these gages. Figure 10 and 11 show the recorded pressures from these gages for two firing of 0.454 kg (1 lb) charges at a height-of-burst corresponding to $Z = 0.2$ m/kg$^{1/3}$ (0.5 ft/lb$^{1/3}$). While some evidence of ringing of the armor plate may be present in these records, they serve to provide insight into the complexities of blast wave reflections at small Z. Figure 10 illustrates the variability of wave forms for normal reflection which may occur for nominally identical firings. For this case the tables of Kingery and Pannill[7] gave a peak reflected overpressure of 168.68 MPa (24465 psi) while Jack[13] has reported the value 186.4 MPA

[13]W. H. Jack, Jr., "Measurements of Normally Reflected Shock Waves from Explosive Charges," Ballistic Research Laboratories Memorandum Report No. 1499, July 1963.

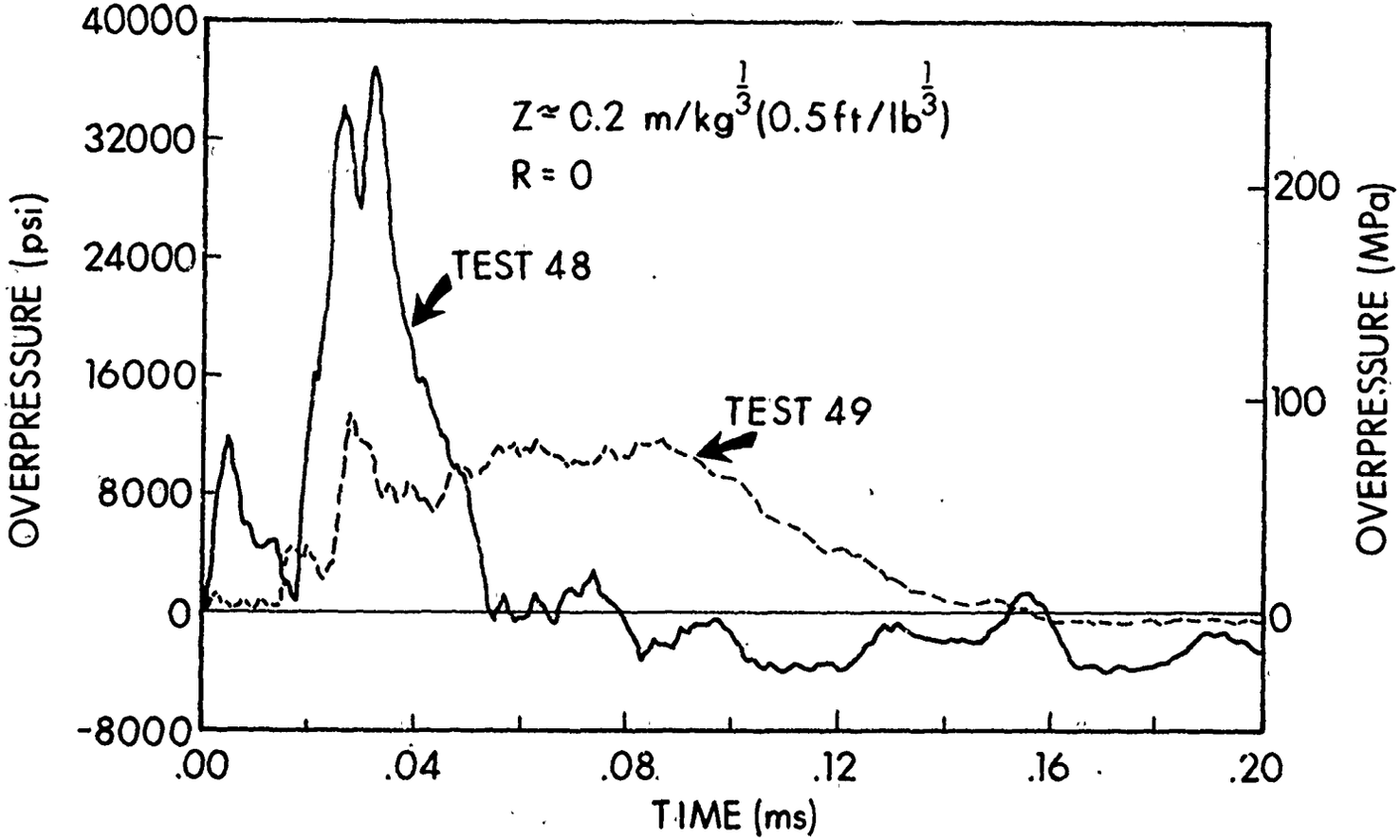

Figure 10. Comparison of Normally Reflected Overpressure Records

(27040 psi) as the average of three firings using 0.057 kg (1/8 lb) charges. In Figure 11 the reflected overpressure records for the same two firings are seen to be in much closer agreement. The location of this gage with respect to "ground zero" is just outside of the regular reflection zone.

For the same charge weight a single firing was made at $Z = 0.12$ m/kg$^{1/3}$ (0.3 ft/lb$^{1/3}$); the blast overpressure recorded at the same two gage locations are shown in Figures 12 and 13, respectively. The very high pressures shown in Figure 12 resulted in damage to this gage; it is not clear whether the true peak reflected pressure was reached before this occurred. According to Kingery and Pannill[7] one would expect a peak reflected pressure of only 348.0 MPa (50,476 psi). However, Kulesz et al[6] have reported an experimental value of 830 MPa (120,000 psi) for this case. Interpolating data from this source one would estimate a peak pressure of 210 MPa (30,000 psi) for the location of the gage output shown in Figure 13, which is clearly not the result obtained. Owing to the decreased height-of-burst this location is a bit further into the Mach reflection region than was the case for Figure 11.

The blast pressure measurements reported in Figures 10-13 are too few in number to have any statistical significance but do indicate that uncertainties associated with blast load predictions increase rapidly as Z is reduced. More importantly, it should be noted that none of these blast pulses have the sharp rise followed by exponential decay that is typical at larger scaled distances. These anomalous wave forms pose serious problems in the evaluation of such blast parameters as positive phase duration and positive impulse.

The determination of the reflected positive duration was a prime objective of these pressure measurements since this is required for estimation of plug motion during the blast pulse. The displacement at the end of the blast pulse is given by Equation (A-6) where, for short pulses, the first term is negligible in comparison to the second. C is a non-dimensional pulse shape factor which, for the shapes considered in Appendix A, is in the range $\frac{1}{2} \leq C \leq 1$. Thus, for a specified velocity $\dot{x}_o$, the displacement x(T) is directly proportional to T. Although data on positive duration for small Z are rather sparse it appears[14] that this quantity is nearly constant over the range $0.08 \leq Z \leq 0.20$ m/kg$^{1/3}$ ($0.15 \leq Z \leq 0.50$ ft/lb$^{1/3}$) and is of the order of 0.13 ms/kg$^{1/3}$ (0.1 ms/lb$^{1/3}$), consistent with the positive durations seen in Figures 10-13. On this basis it is felt that the plug motion during the blast pulse may have been somewhat greater than anticipated for tests at the smallest scaled distances.

---

[14] C. N. Kingery and G. Bulmash, "Airblast Parameters from TNT Spherical Air Burst and Hemispherical Surface Burst," Ballistic Research Laboratory Technical Report ARBRL-TR-02555, April 1984.

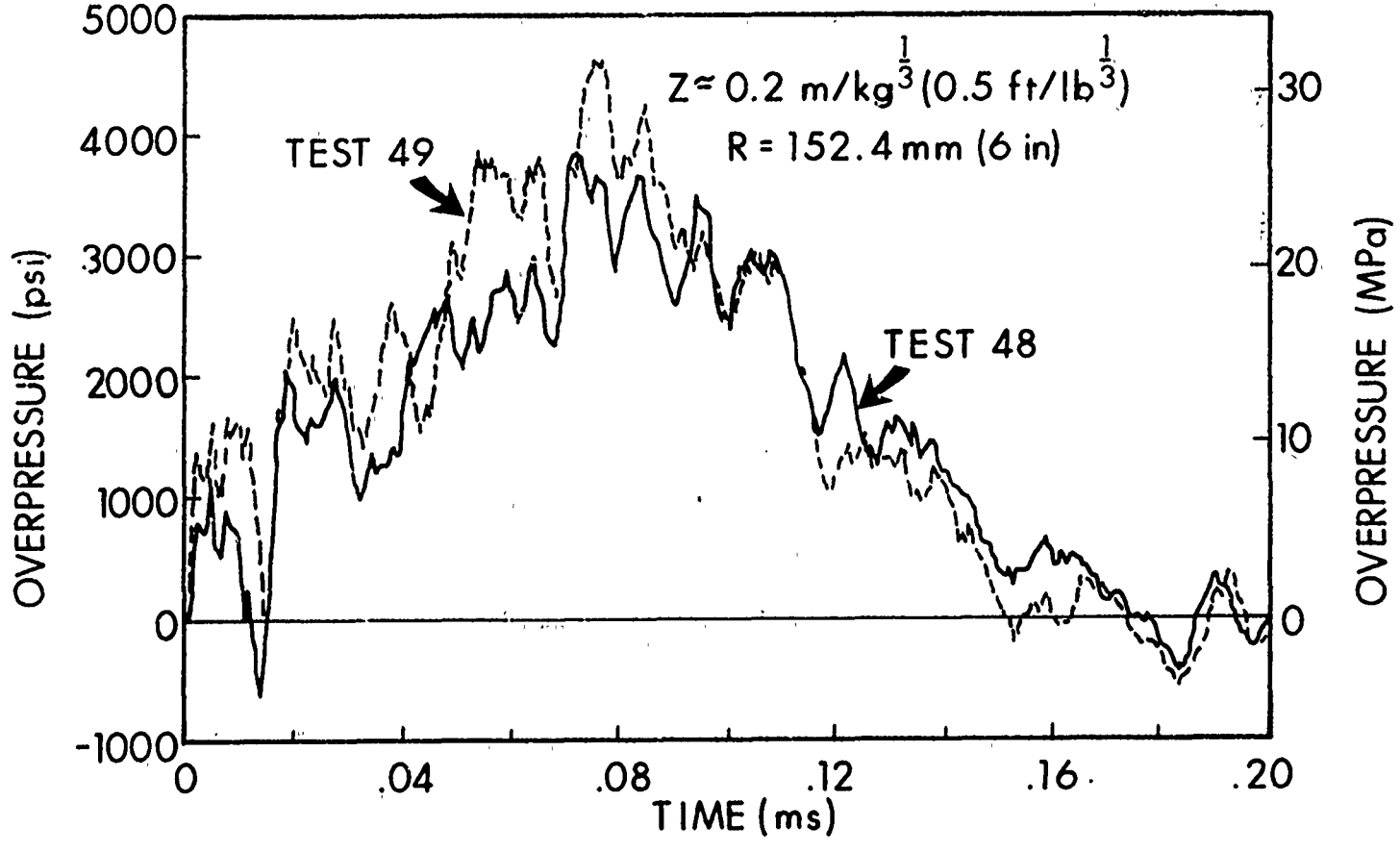

Figure 11. Comparison of Reflected Overpressures in Mach Region

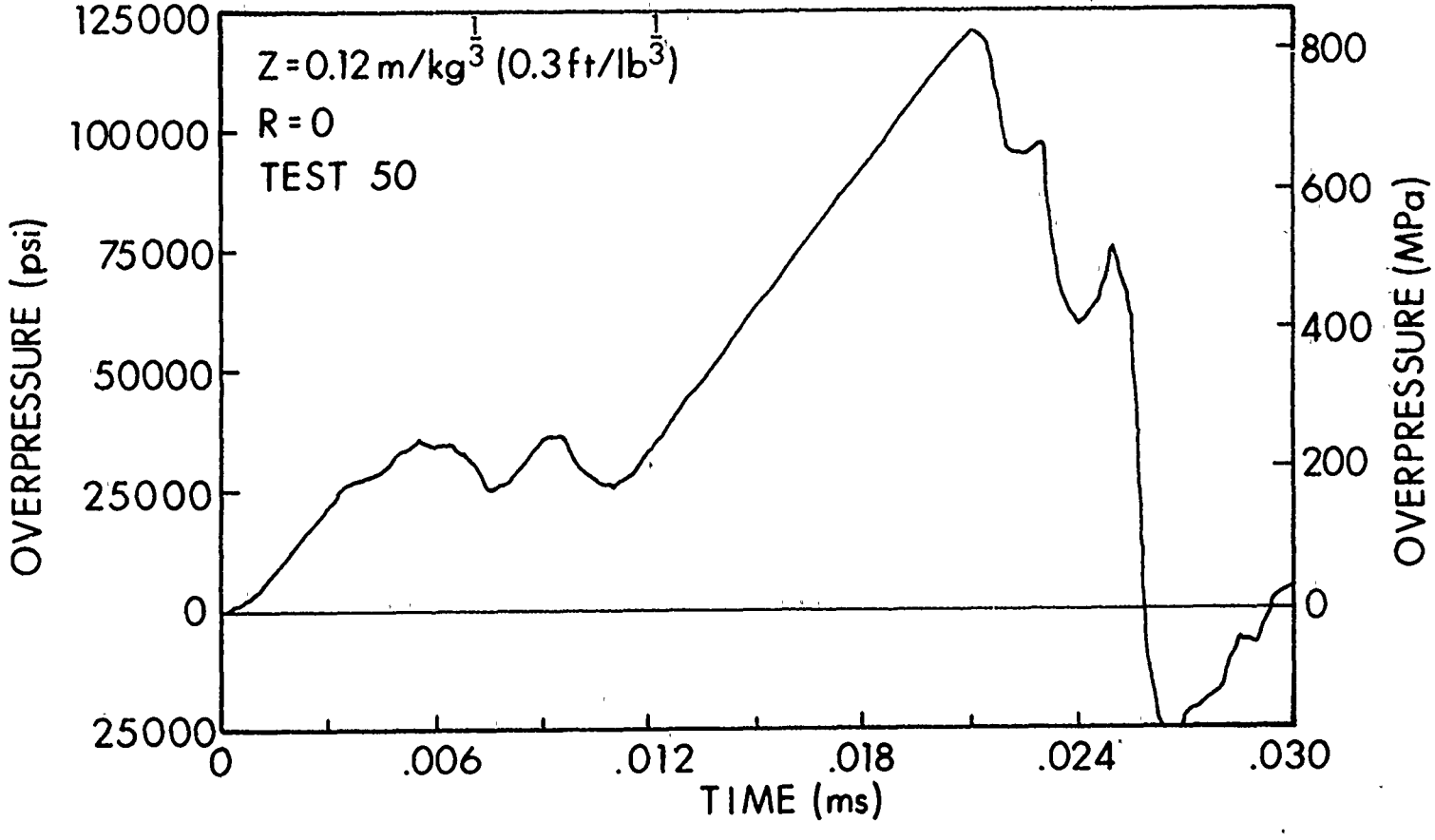

Figure 12. Normally Reflected Overpressure at Smaller Z

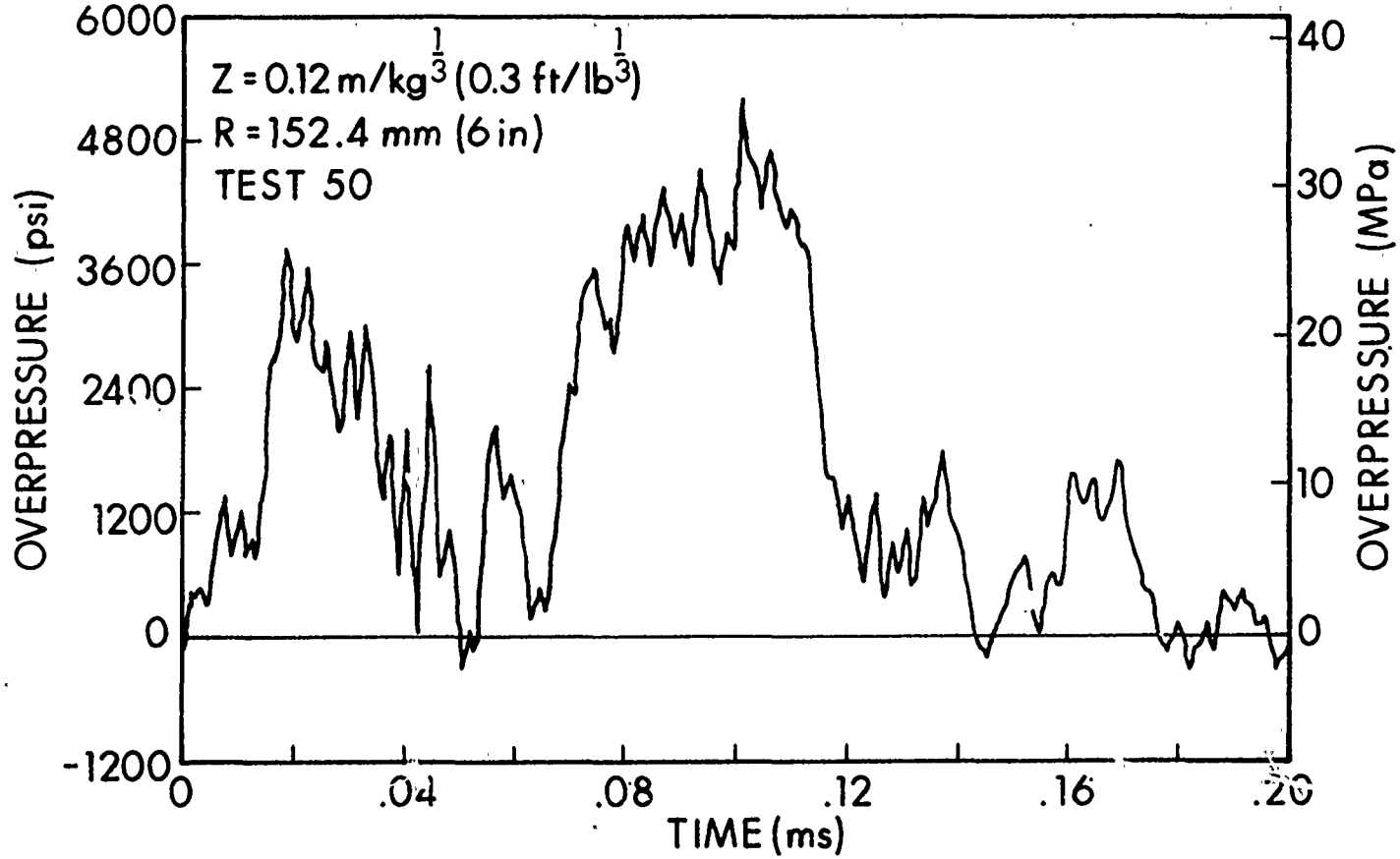

Figure 13. Mach Reflected Overpressure at Same Z

IV. CONCLUDING REMARKS

Data on normally reflected impulse from spherical Pentolite charges have been presented for the range of small scaled distances not adequately treated in the literature. Although the experimental measurements are believed to be normally distributed the effects omitted in the interpretive analysis: mechanical friction, air drag, and pressure relieving motion of the plug during the positive phase of the blast pulse all would tend to reduce the plug velocity. Consequently, the reported values should represent a (hopefully close) lower bound to the normally reflected impulse which an infinite rigid plane would experience.

There is tentative evidence that the Hopkinson scaling law (and consequentially, Sachs' scaling) may become inapplicable for $Z < 0.16$ m/kg$^{1/3}$ (0.4 ft/lb$^{1/3}$). Further evaluation of this matter using a greater variation of charge weights is needed.

The experimental difficulties encountered in this program were described, as were the corrective measures which were undertaken. For future testing a reliable method for measuring the transient velocity of the plug should be established as well as a means of determining the pulse duration. Provision for simultaneous recording of surface pressures as a function of distance R should be made; these are needed for structural response calculations.

With respect to the comparison of impulses shown in Figure 2, the experimental value from Test No. 89 may be included at $R/H = 0$. From Table B-2 one finds $I = 51.3$ kpa·s (7440 psi-ms), which is somewhat less than the empirical values shown in Figure 2. Although there is only a single data point for this case it may be seen from Figure 8 that it is consistent with those for neighboring values of Z. Therefore it may be concluded that the normally reflected impulse derived from the HULL hydrocode is not more than 60% of the best available experimental value. It is hoped that refinements to the modeling of the detonation process and of the treatment of explosive products can be devised which will bring the hydrocode predictions into line with the experimental evidence. This is sorely needed since computational hydrodynamics can provide detail regarding spatial distribution of pressure and impulse which is infeasible to obtain experimentally.

ACKNOWLEDGMENTS

Numerous individuals provided assistance during the conduct of this investigation and the authors wish to express their thanks to all who participated. R. Lottero provided the HULL code solution referenced herein. M. Saccucci helped with the statistical design of the experiments. W. T. Robinson assisted with performance of the experiments and with collection of information to be included in the report. R. Schumacher provided support for data reduction and plotting. C. N. Kingery provided extrapolated data from experiments performed by Southwest Research Institute and, during the

review of this report, called attention to a relevant paper by Baker[15] which is taken into consideration in Appendix C. G. Bulmash assisted with calculations related to the Baker paper. Finally, O. T. Johnson and R. Shear participated in helpful discussions with the principal author.

[15]W. E. Baker, "Prediction and Scaling of Reflected Impulse from Strong Blast Waves," International Journal of Mechanical Sciences, Vol. 9, 1967, pp. 45-51.

REFERENCES

1. B. Hopkinson, British Ordnance Board Minutes 13565, 1915.

2. O. T. Johnson, J. D. Patterson II, and W. C. Olson, "A Simple Mechanical Method for Measuring the Reflected Impulse of Air Blast Waves," Ballistic Research Laboratories Memorandum Report No. 1088, July 1957.

3. H. J. Goodman, "Compiled Free-Air Blast Data on Bare Spherical Pentolite," Ballistic Research Laboratories Report No. 1092, February 1960.

4. W. C. Olson, J. D. Patterson II, and J. S. Williams, "The Effect of Atmospheric Pressure of the Reflected Impulse from Air Blast Waves," Ballistic Research Laboratories Memorandum Report No. 1241, January 1960.

5. R. G. Sachs, "The Dependence of Blast on Ambient Pressure and Temperature," Ballistic Research Laboratory Report No. 466, May 1944.

6. J. J. Kulesz, E. D. Esparza, and A. B Wenzel, " Blast Measurements at Close Standoff Distances for Various Explosive Geometries," Minutes of the Eighteenth Explosives Safety Seminar, Vol. I, pp. 405-445, September 1978.

7. C. N. Kingery and B. F. Pannill, "Parametric Analysis of the Regular Reflection of Air Blast," Ballistic Research Laboratories Report No. 1249, June 1964.

8. R. Courant and K. O. Friedrichs, "Supersonic Flow and Shock Waves," Interscience Publishers, New York, 1948, pp. 327-331.

9. D. A. Matuska and R. E. Durrett, "The HULL Code, A Finite Difference Solution to the Equations of Continuum Mechanics," AFATL-TR-78-125, November 1978.

10. B. Soroka, "Air Blast Tables for Spherical 50/50 Pentolite Charges at Side-On and Normal Incidence," Ballistic Research Laboratory Memorandum Report ARBRL-MR-02975, December 1979.

11. G. R. Moore, "Calculations of the Reflected Overpressure and Transient Loading on a Deck from Elevated Gun Fire," Naval Weapons Laboratory Technical Report TR-2847, November 1972.

12. M. G. Natrella, Engineering Design Handbook, Experimental Statistics, Section 4, Chapter 17, AMCP 706-113, March 1966.

13. W. H. Jack, Jr., "Measurements of Normally Reflected Shock Waves from Explosive Charges," Ballistic Research Laboratories Memorandum Report No. 1499, July 1963.

14. C. N. Kingery and G. Bulmash, "Airblast Parameters from TNT Spherical Air Burst and Hemispherical Surface Burst," Ballistic Research Laboratory Technical Report ARBRL-TR-02555, April 1984.

15. W. E. Baker, "Prediction and Scaling of Reflected Impulse from Strong Blast Waves," International Journal of Mechanical Sciences, Vol. 9, 1967, 45-51.

LIST OF SYMBOLS

A	area of (circular) cross section of plug
C	pulse shape factor
H	height-of-burst (to center of sphere)
I	impulse per unit area
K	coefficient in Equation (C-2), $= \sqrt{2Y/M_E}/4\pi g$
M_E	mass of explosive charge
M_A	mass of air engulfed by shock wave
R	horizontal radial distance to "ground zero"
T	duration of positive phase of blast pulse
W	weight of spherical explosive charge
Y	energy released by M_E
Z	Hopkinson scaled distance ($= H/W^{1/3}$)
g	acceleration of gravity
m	mass of plug
p	transient reflected pressure
p_o	peak reflected pressure
t	time
x	vertical position of mass center of plug relative to its initial position
$\dot{x}_o$	velocity imparted to plug by blast alone ($= AI/m$)
β	decay coefficient of the Friedlander pulse
γ	ratio of specific heats ($= c_p / c_v$)
σ	standard deviation
τ	dummy time variable

APPENDIX A

ANALYSIS OF IMPULSE PLUG RESPONSE

APPENDIX A
ANALYSIS OF IMPULSE PLUG RESPONSE

If the effect of air resistance is neglected, the motion of the plug in the presence of the gravitational field is described by the differential equation

$$m\ddot{x} = A\,p(t) + mg \tag{A-1}$$

subject to the initial conditions

$$x(0) = 0\,,\ \dot{x}\,(0) = 0 \tag{A-2}$$

Equation (A-1) may be successively integrated to obtain expressions for the velocity and the displacement:

$$\dot{x}(t) = gt + \frac{A}{m}\int_o^t p(\tau)d\tau \tag{A-3}$$

$$x(t) = \frac{1}{2}gt^2 + \frac{A}{m}\int_o^t p(\tau)\,(t-\tau)\,d\tau \tag{A-4}$$

In order to proceed further one must be more specific regarding the form of p(t). Three possible pulse shapes were considered in this investigation:

(1) a linearly decaying (triangular) pulse, which had been employed by Johnson, Patterson, and Olson;
(2) the Friedlander function, which is often used to represent the classical decay of a blast wave; and
(3) a half-sine pulse, which was included in view of the non-classical pressure records observed experimentally for small Z.

Figure A-1 presents sketches of the pulses and the associated analytical formulations for the transient pressures.

For any blast pulse where the response of the plug is described by Equation (A-1) the velocity at the end of the pulse is:

$$\dot{x}(T) = gT + \frac{AI}{m} \tag{A-5}$$

Let $\dot{x}_o = \dfrac{AI}{m}$ be the velocity imparted to the plug by the blast pulse in the absence of a gravitational field. Then, the displacement of the plug at the end of the pulse is given by:

$$x\,(T) = \frac{1}{2}gT^2 + CT\,\dot{x}_o \tag{A-6}$$

where the dependence on pulse shape is incorporated in the factor C which has the values $\dfrac{2}{3}$, $\dfrac{2-2\beta+\beta^2-2e^{-\beta}}{\beta(e^{-\beta}-1+\beta)}$, $\dfrac{1}{2}$, respectively, for the three pulses presented in Figure A-1. The velocities and displacements of the plug after the end of the pulse are given by:

Triangular Pulse

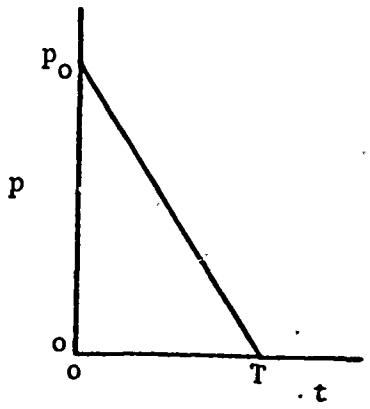

$$p(t) = \begin{cases} p_o\left(1 - \frac{t}{T}\right) & o \leq t \leq T \\ o & t > T \end{cases}$$

$$I = p_o T/2$$

Friedlander Pulse

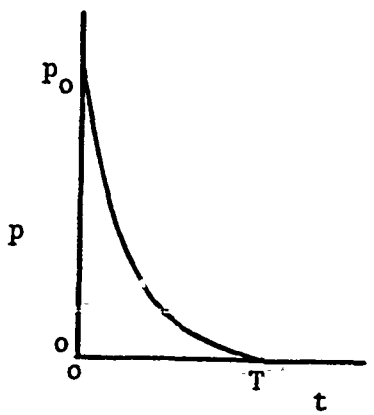

$$p(t) = \begin{cases} p_o\left(1 - \frac{t}{T}\right)e^{-\frac{\beta t}{T}} & o \leq t \leq T \\ o & t \geq T \end{cases}$$

$$I = p_o T\,(e^{-\beta} - 1 + \beta)/\beta^2$$

Half-Sine Pulse

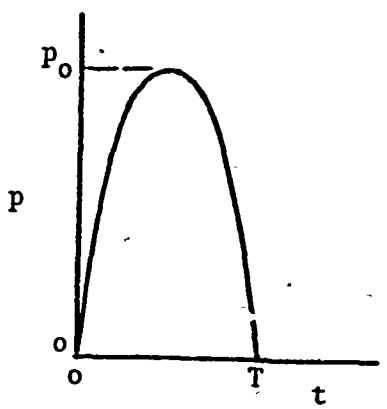

$$p(t) = \begin{cases} p_o \sin\frac{\pi t}{T} & o \leq t \leq T \\ o & t > T \end{cases}$$

$$I = 2p_o T/\pi$$

Figure A-1. Pulse Shapes Considered in the Analysis

$$\left.\begin{aligned} \dot{x} &= gt + \dot{x}_o \\ x &= \frac{1}{2}gt^2 + \dot{x}_o\, t + (C-1)\dot{x}_o\, T \end{aligned}\right\} \quad t \geq T \qquad \begin{matrix}(A\text{-}7)\\(A\text{-}8)\end{matrix}$$

Equation (A-8) provides expressions for plug locations x_1 , x_2 at times t_1 , t_2, where $t_2 > t_1 > T$. Taking the difference of these expressions one obtains:

$$\dot{x}_o = \frac{x_2 - x_1}{t_2 - t_1} - \frac{g}{2}(t_2 + t_1) \qquad (A\text{-}9)$$

This relation, while valid, has the disadvantage that the times t_1 and t_2 from the arrival of the blast pulse at the plug must be known. Since it is easier experimentally to measure $t_2 - t_1$, write:

$$\dot{x}_1 = gt_1 + \dot{x}_o \qquad (A\text{-}10)$$

and substitute for $\dot{x}_o$ from (A-9) to obtain:

$$\dot{x}_1 = \frac{x_2 - x_1}{t_2 - t_1} - \frac{g}{2}(t_2 - t_1) \qquad (A\text{-}11)$$

Time can be eliminated between Equations (A-7) and (A-8) (written for $t = t_1$) to obtain a quadratic expression in $\dot{x}_o$ which yields:

$$\dot{x}_o = \sqrt{\dot{x}_1^2 - 2gx_1 + (1-C)^2 g^2 T^2} - (1-C)\, gT \qquad (A\text{-}12)$$

In order to employ Equation (A-12) one needs the value of the pulse duration T (which was not measured in the plug experiments). Data on normally reflected positive duration published by Jack[13] indicate a monotonic decrease of duration with Z but no values were given for $Z < 0.4$ m/kg$^{1/3}$ (1 ft/lb$^{1/3}$). The durations observed in the three pressure measurement tests reported herein were all a small fraction of a millisecond. A study was conducted using representative data from this report in Equation (A-12), taking T to be both 0 and 1 ms. The difference in the velocity was found to be of the order of 0.01% or less so it was concluded that the terms involving T could be omitted from Equation (A-12) for the present application. On this basis the value of impulsive velocity is given by:

$$\dot{x}_o = \sqrt{\dot{x}_1^2 - 2gx_1} \qquad (A\text{-}13)$$

with the value of $\dot{x}_1$ obtained from Equation (A-11). These results provide the basis for Equation (2) of this report.

APPENDIX B

EXPERIMENTAL MEASUREMENTS AND UNSCALED RESULTS

APPENDIX B

EXPERIMENTAL MEASUREMENTS AND UNSCALED RESULTS

Table B-1 is a listing of the basic data obtained in each test, given in the units actually employed in the measurements. Results of some intermediate calculations are listed in Table B-2. Tabulated in both metric S.I. and English units are the plug velocity at the end of the pulse and the corresponding impulse (per unit area).

TABLE B-1. SUMMARY OF TEST DATA

Test No.	Charge Weight W grams	H in.	Plug Weight grains	Plug Diameter in.	x_1 in.	x_2 in.	t_1 ms	t_2 ms
33	479.7	6.134	384.5	.4985	13.8	31.3	12.58	28.04
34	483.5	6.134	384.5	.4985	13.9	31.6	12.52	27.90
35	487.0	6.134	384.5	.4985	13.6	31.3	12.32	27.72
36	488.0	6.134	384.5	.4985	13.7	31.2	12.40	27.78
37	490.0	6.134	384.5	.4985	13.7	31.2	12.60	28.02
38	484.4	4.915	384.5	.4985	14.2	32.3	8.66	19.13
39	485.5	4.915	384.5	.4985	14.3	32.2	8.60	19.14
40	485.9	4.915	384.5	.4985	14.2	32.3	8.69	19.26
41	488.9	4.915	384.5	.4985	14.3	32.4	8.65	19.21
42	490.9	4.915	384.5	.4985	14.2	32.4	8.67	19.23
43	480.0	3.687	384.5	.4985	13.6	33.8	4.86	11.73
44	480.4	3.687	384.5	.4985	13.9	33.7	4.98	11.88
45	484.8	3.687	384.5	.4985	14.1	34.0	4.97	11.84
52	487.3	3.687	388.	.4995	14.8	30.9	5.64	11.59
54	481.7	3.687	388.	.4995	15.9	33.3	5.70	11.62
56	484.9	3.687	388.	.4995	15.8	34.0	5.69	11.83
65	896.5	7.5252	389.	.4995	16.3	35.5	12.38	26.38
66	897.7	7.5252	389.	.4995	13.5	30.8	10.48	23.26
67	899.1	7.5252	389.	.4995	13.8	31.5	10.38	23.06
68	887.7	7.5252	389.	.4995	14.1	31.8	10.62	23.22
69	896.6	7.5252	389.	.4995	13.3	30.0	10.64	23.22
70	893.8	6.024	389.	.4995	13.1	31.8	6.64	15.54
71	896.2	6.024	389.	.4995	13.0	31.3	6.68	15.64
72	898.1	6.024	389.	.4995	13.2	31.8	6.70	15.67
74	869.9	6.024	389.	.4995	12.4	29.4	6.66	15.57
75	893.3	6.024	389.	.4995	13.0	31.4	6.66	15.55

TABLE B-1. SUMMARY OF TEST DATA (CONT'D)

Test No.	Charge Weight W grams	H in.	Plug Weight grains	Plug Diameter in.	x_1 in.	x_2 in.	t_1 ms	t_2 ms
76	872.2	4.515	389.	.4995	15.1	29.1	4.70	8.81
77	886.4	4.515	389.	.4995	16.0	30.7	4.74	8.83
78	894.2	4.515	389.	.4995	16.3	30.9	4.765	8.85
79	895.6	4.515	389.	.4995	16.1	30.8	4.70	8.81
80	897.4	4.515	389.	.4995	16.0	30.8	4.72	8.845
83	893.0	3.010	380.	.4968	35.3	52.25	4.63	6.81
84	896.1	3.010	380.	.4968	36.0	52.8	4.64	6.80
87	897.5	3.010	386.	.4997	36.5	52.3	4.735	6.845
89	895.6	2.489	387.	.4985	33.2	47.4	3.05	4.45
92	485.0	2.461	384.	.4978	36.0	51.7	5.715	8.165
93	487.0	2.461	384.	.4978	34.1	53.5	5.24	8.175
95	489.9	2.461	384.	.4978	30.5	50.2	4.705	7.66
96	479.1	2.461	384.	.4978	30.0	49.6	4.74	7.725
97	483.5	2.461	384.	.4978	30.8	50.9	4.73	7.735
98	227.8	3.877	384.	.498	28.7	43.7	23.02	34.46
99	238.5	3.877	384.	.498	29.1	44.6	23.12	34.74
100	238.6	3.877	384.	.498	30.4	46.1	23.04	34.54
101	239.8	3.877	384.	.498	29.5	45.1	23.16	34.7
102	240.0	3.877	384.	.498	28.7	44.1	23.16	34.7
103	228.0	2.908	384.	.498	31.0	46.7	13.47	20.0
104	237.7	2.908	384.	.498	31.3	47.6	13.46	20.07
107	243.3	2.908	384.	.498	31.5	47.7	13.48	20.05
109	241.1	2.908	384.	.498	31.4	47.4	13.65	20.25
110	241.7	2.908	384.	.498	31.5	47.1	13.64	20.21
111	241.9	1.938	384.	.498	34.5	51.8	6.85	10.18
112	242.2	1.938	384.	.498	29.8	47.0	5.865	9.185
113	227.4	1.909	384.	.498	30.5	48.6	5.80	9.095
114	227.9	1.909	384.	.498	29.9	47.4	5.82	9.12
115	228.0	1.909	384.	.498	31.8	50.2	5.84	9.155
116	238.7	1.454	383.	.497	32.8	48.1	3.955	5.71
125	242.3	1.454	385.	.498	30.2	44.9	3.95	5.70

TABLE B-2. PLUG VELOCITIES AND UNSCALED IMPULSES

Test No.	$\dot{x}_o$ m/s	$\dot{x}_o$ in/ms	I kpa·s	I psi·ms
33	28.5	1.124	5.65	820.
34	29.0	1.143	5.75	833.
35	29.0	1.142	5.74	832.
36	28.7	1.130	5.68	824.
37	28.6	1.127	5.67	822.
38	43.8	1.724	8.66	1257.
39	43.0	1.693	8.51	1234.
40	43.4	1.707	8.58	1245.
41	43.4	1.709	8.59	1246.
42	43.6	1.718	8.64	1253.
43	74.6	2.94	14.76	2140.
44	72.8	2.87	14.41	2090.
45	73.5	2.89	14.54	2110.
52	68.6	2.70	13.65	1980.
54	74.6	2.94	14.93	2150.
56	75.2	2.96	14.96	2170.
65	34.6	1.364	6.91	1002.
66	34.2	1.347	6.82	990.
67	35.3	1.390	7.04	1021.
68	35.5	1.398	7.08	1027.
69	33.6	1.321	6.69	971.
70	53.3	2.10	10.62	1540.
71	51.8	2.04	10.32	1497.
72	52.6	2.07	10.48	1520.
74	48.4	1.904	9.64	1399.
75	52.5	2.07	10.46	1517.
76	86.5	3.40	17.24	2500.
77	91.2	3.59	18.19	2640.
78	90.7	3.57	18.09	2620.
79	90.8	3.57	18.10	2620.
80	91.1	3.59	18.16	2630.
83	197.4	7.77	38.9	5640.
84	197.5	7.78	38.9	5640.
87	190.1	7.49	37.6	5450.
89	258.	10.14	51.3	7440.

TABLE B-2. PLUG VELOCITIES AND UNSCALED IMPULSES (CONT'D)

Test No.	$\dot{x}_o$ m/s	$\dot{x}_o$ in/ms	I kpa·s	I psi·ms
92	162.7	6.41	32.2	4680.
93	167.8	6.61	33.3	4820.
95	169.3	6.66	33.5	4870.
96	166.7	6.56	33.0	4790.
97	171.0	6.73	33.9	4910.
98	33.0	1.300	6.54	949.
99	33.6	1.323	6.66	965.
100	34.4	1.354	6.81	988.
101	34.1	1.341	6.75	978.
102	33.6	1.324	6.66	966.
103	60.9	2.40	12.06	1749.
104	62.5	2.46	12.37	1795.
107	62.5	2.46	12.37	1794.
109	61.4	2.42	12.16	1764.
110	60.1	2.37	11.91	1728.
111	131.9	5.19	26.1	3790.
112	131.5	5.18	26.0	3780.
113	139.5	5.49	27.6	4010.
114	134.6	5.30	26.7	3870.
115	140.9	5.55	27.9	4050.
116	221.	8.72	43.9	6370.
125	213.	8.40	42.4	6140.

APPENDIX C

CORRELATIONS WITH PREDICTIONS EMPLOYING BAKER'S MODEL

APPENDIX C
CORRELATIONS WITH PREDICTIONS EMPLOYING BAKER'S MODEL

W. E. Baker[15] recommends the semi-empirical formula

$$I = \sqrt{2(M_E + M_A)\, Y} \;/\; 4\,\pi\, H^2 \qquad \text{(C-1)}$$

for prediction of the normally reflected impulse imparted to a rigid wall. He also shows that for $M_A << M_E$. Equation (C-1) is consistent with Hopkinson's scaling law and that a reasonable upper limit on Z for neglect of M_A is 0.269 $m/kg^{1/3}$ (0.679 $ft/lb^{1/3}$). If M_A can be neglected Equation (C-1) can be readily manipulated into the form

$$I / W^{1/3} = K / Z^2 \qquad \text{(C-2)}$$

where K is a dimensional coefficient which can be adjusted to match data for impulse delivered by specific explosives. Using the data of this report for 50/50 Pentolite at Z = 0.2 $m/kg^{1/3}$ (0.5 $ft/lb^{1/3}$) one obtains:

$$I / W^{1/3} = \begin{cases} 0.2833 / Z^2 & \text{in S. I. units} \\ 200.65 / Z^2 & \text{in English units} \end{cases} \qquad \text{(C-3)}$$

This simple inverse square dependence on Z has been employed to predict values of scaled impulse corresponding to the mean experimental values shown in Table 1. The values of $I/W^{1/3}$ obtained from Equation (C-3) and the percent differences from the corresponding experimental data are listed in Table C-1. It may be seen that Baker's procedure provides values of reflected impulse which are quite satisfactory except for the very small Z range where it has already been concluded that Hopkinson scaling may become inapplicable.

TABLE C-1. SCALED IMPULSES DERIVED FROM EQUATION (C-3)

Z		Nominal Charge Wt.	$I/W^{1/3}$		%Difference
$m/kg^{1/3}$	$ft/lb^{1/3}$	lb	$kpa \cdot s/kg^{1/3}$	$psi \cdot ms/lb^{1/3}$	from Exp. Value
0.1982	0.4997	1.0	7.212	803.6	-0.5
0.1983	0.4999	2.0	7.204	802.9	0.5
0.1592	0.4012	0.5	11.178	1246.6	3.5
0.1587	0.4000	1.0	11.248	1254.1	3.0
0.1588	0.4002	2.0	11.234	1252.8	3.4
0.1191	0.3003	0.5	19.972	2225.0	1.7
0.1194	0.3010	1.0	19.872	2214.7	6.0
0.1193	0.3006	2.0	19.905	2220.6	6.7
0.0792	0.1997	0.5	45.16	5031.	3.4
0.0796	0.2006	1.0	44.71	4986.	5.8
0.0793	0.1999	2.0	45.05	5021.	12.9
0.0656	0.1653	2.0	65.83	7343.	23.8
0.0594	0.1497	0.5	80.29	8954.	15.8

DISTRIBUTION LIST

No. Of Copies	Organization
12	Administrator Defense Technical Info Center ATTN: DTIC-DDA/ Cameron Station Alexandria, VA 22304-6145
1	HQDA DAMA-ART-M Washington, DC 20310
1	HQDA DAMA-AR-A Washington, DC 20310
1	HQDA DAMA-WSM Washington, DC 20310
1	HQDA DACS-BMZ-A Washington, DC 20310
1	Director of Defense Rsch & Eng ATTN: DD/TWP Washington, DC 20301
1	Asst to the Secretary of Defense (Atomic Energy) ATTN: Document Control Washington, DC 20301
1	Director Defense Advanced Research Projects Agency 1400 wilson Boulevard Arlington, VA 22209
1	Office of Deput Under-Sec of Defense for Rsch & Eng (ET) ATTN: Mr. J. Persh Staff Spec for Materials & Structures Room 3D1089, The Pentagon Washington, DC 20301
2	Federal Emergency Management Agency ATTN: Mr. M. Pachuta RF-SR, Tech Lib Washington, DC 20472

No. of Copies	Organization
2	Chairman Department of Defense Explosives Safety Board RM 856-C, Hoffman Bldg.1 2461 Eisenhower Avenue Alexandria, VA 22331
1	Director Defense Intelligence Agency ATTN: DT-2/Wpns & sys div Washington, DC 20301
1	Director National Security Agency ATTN: E. F. Butala, R15 Ft. George G. Meade, MD 20755
6	Director Defense Nuclear Agency ATTN: STSI/Archives DDST/Dr. Oswald SPAS, SPSS, SPTD, RATN Washington, DC 20305
1	Director Inst for Defense Analyses ATTN: IDA Librarian 1801 Beauregard Street Alexandria, VA 22311
1	Commander US Army Concepts Analysis Agency 8120 Woodmont Avenue Bethesda, MD 20014
1	Deputy Chief of Staff for Intelligence USA-Europe ATTN: Tech Secretary APO, NY 09131
1	Headquarters US Army Europe Tech Intelligence Center ATTN: AEUTTIC Department of the Army APO, NY 09403

DISTRIBUTION LIST

No. of Copies	Organization
1	Commandant US Army Command and General Staff College ATTN: Archives Ft Leavenworth, KS 66027
1	Commander US Army Materiel Command ATTN: AMCD A-ST 5001 Eisenhower Avenue Alexandria, VA 22333-0001
1	Commander Armament R&D Center US Army AMCCOM ATTN: SMCAR-TDC Dover, NJ 07801-5001
1	Commander Armament R&D Center US Army AMCCOM ATTN: SMCAR-TSS Dover, NJ 07801-5001
1	Commander US Army Armament, Munitions and Chemical Command ATTN: SMCAR-ESP-L Rock Island, IL 61299
1	Director Benet Weapons Laboratory Armament R&D Center US Army AMCCOM ATTN: SMCAR-LCB-TL Watervliet, NY 12189
2	Commander US Army Armament Materiel Readiness Command ATTN: AMCPM-ARGADS AMSMC-RDF Rock Island, IL 61299
2	Dep Chief of Staff for Operations & Plans ATTN: Tech Lib Dir, Chem Nuc Operations Department of Army Washington, DC 20310
1	Director US Army BMD Adv Tech Center P.O. Box 1500 Huntsville, AL 35807
1	Commander US Army BMD Command ATTN: BDMSC-TEN (N. Hurst) P.O. Box 1500 Huntsville, AL 35807
2	Office, Chief of Engineers Department of Army ATTN: DAEN-MCE-D DAEN-RDM 300 S. Pickett St Alexandria, VA 22304
3	Commander US Army Aviation Research and Development Command ATTN: AMSAV-E AMSAV-DI AMSAV-ASE 4300 Goodfellow Blvd St. Louis, MO 63120
1	Director US Army Air Mobility Research and Development Laboratory Ames Research Center Moffett Field, CA 94035
4	Director Applied Technology Lab US Army Research & Technology Development Laboratory ATTN: AMDDL-EU-VAT/Mr. Merritt AMDDL-PP/Mr. Morrow AMDDL-ATL AMDDL-RM Fort Eustis, VA 23604

DISTRIBUTION LIST

No. of Copies	Organization
1	Commandant US Army Troop Support & Aviation Material Readiness Command ATTN: AMSTG-G/Sys Anal Ofc 4300 Goodfellow Boulevard St. Louis, MO 63120
1	Commander US Army Communications - Electronics Command ATTN: AMSEL-ED Fort Monmouth, NJ 07703
1	Commander US Army Engineer Waterways Exp Station ATTN: Tech Lib P.O. Box 631 Vicksburg, MS 39180
1	Commander US Army Eng Center Fort Belvoir, VA 22060
1	Commander US Army MERADCOM ATTN: AMDME-EM, D. Frink Fort Belvoir, VA 22060
1	Director US Army Electronics R&D Command ATTN: DELET-D Fort Monmouth, NJ 07703
1	Commander US Army Electronics Research and Development Command Technical Support Activity ATTN: DELSD-L Fort Monmouth, NJ 07703
5	Commander US Army Harry Diamond Lab ATTN: L. Belliveau R. Bostak J. Gaul J. Gwaltney R. Kinamer J. Meszaros 2800 Powder Mill Road Adelphi, MD 20783
1	Commander US Army Foreign Science & Technology Center ATTN: Research & Concepts Branch Federal Office Building 220 7th Street, NE Charlottsville, VA 22901
1	Commander US Army Missile Command ATTN: AMCPM-MDET-PA Redstone Arsenal, AL 35898
1	Commander US Army Missile Command ATTN: AMCPM-HA Redstone Arsenal, AL 35898
1	Commander US Army Missile Command ATTN: AMCPM-SHO-E Redstone Arsenal, AL 35898
1	Commander US Army Missile Command ATTN: AMSMI-R Redstone Arsenal, AL 35898
1	Commander US Army Missile Command ATTN: AMSMI-YDL Redstone Arsenal, AL 35898
1	Commander US Army Missile Command ATTN: AMSMI-CM Redstone Arsenal, AL 35898

DISTRIBUTION LIST

No. of Copies	Organization
1	Commander US Army Belvior R&D Center ATTN: AMDME-NC Fort Belvoir, VA 22060
1	Commander US Army Research Office P.O. Box 12211 Research Triangle Park, NC 27709
4	Commander US Army Natick Research & Development Command ATTN: STRNC/Dr. D. Sieling STRNC-JE/A. Johnson A. Murphy W. Crenshaw Natick, MA 01762
1	Commander US Army Tank Automotive Command ATTN: AMSTA-TSL Warren, MI 48090
2	Commander US Army Tank Automotive Command ATTN: AMSTA-UL AMSTA-RWL Warren, MI 48090
4	Commander US Army Nuclear & Chemical Agency ATTN: ACTA-NAW MONA-NE Technical Library MAJ Uecke 7500 Backlick Road, Bldg. 2073 Springfield, VA 22150
6	Director US Army Materials and Mechanics Research Center ATTN: AMXMR-RD (Tech Lib) (J. Mescall) (R. Shea) (S.C. Chou) AMXMR-ER (J. Prifti) (Eugene de Luca) Watertown, MA 02172

No. of Copies	Organization
1	Director US Army TRADOC Systems Analysis Activity ATTN: ATAA-SL White Sands Missile Range, NM 88002
1	Commander US Army Training & Doctrine Command Fort Monroe, VA 23615
1	Commandant US Army Air Defense Artillery School ATTN: Air Defense Agency Bldg 5300 Fort Bliss, TX 79916
1	Interscience Nuclear Weapons School ATTN: Technical Library Kirtland AFB, NM 87117
1	Commandant US Army Armor School ATTN: Armor Agency Fort Knox, KY 40121
1	Commandant US Army Aviation School Fort Rucker, AL 36360
2	Commandant US Army Infantry School ATTN: ATSH-CD-CSO-OR Fort Benning, GA 31905
1	Commandant US Army Transportation Corps School Fort Eustis, VA 23604
1	Commander US Army Development & Employment Agency ATTN: MODE-TED-SAB Fort Lewis, WA 98433

DISTRIBUTION LIST

No. of Copies	Organization
1	Commander US Army Combined Arms Combat Dev Activity Ft Leavenworth, KS 66027
1	Commander US Army Air Defense Human Research Unit ATTN: ATHRD Fort Bliss, TX 79916
1	Commander US Army Agency for Aviation Safety Fort Rucker, AL 36360
1	Chief of Naval Operations Department of the Navy Washington, DC 20350
1	Chief of Naval Materiel Department of the Navy Washington, DC 20350
10	Commander Naval Air Systems Command ATTN: Air-5204 (2 cys) Air-605 (3 cys) Air-530 Air-995A Air-536038 Air-330 Air-350 Washington, DC 20360
1	Commander Naval Air Development Center, Johnsville ATTN: SAED, Code 5033 Warminster, Pa 18974
4	Commander Naval Surface Weapons Center ATTN: Code DG-13 Code G-10 Lib Br, DX-21 Dr. J. Soper Dahlgren, VA 22448
4	Commander Naval Surface Weapons Center ATTN: Code 040, Code N- Code 433, Code N- Code WX21/Tech Lib Code WA501 Silver Spring, MD 20910
1	Director Naval Strategic Systems Project Officer ATTN: NSP-43, Tech Lib Munitions Bldg, Rm 3245 Washington, DC 20375
4	Commander Naval Weapons Center ATTN: Code 3431, Tech Lib Code 31804, M. Keith Code 533, Tech Lib Code 6031, Dr. Stronge China Lake, CA 93555
1	Commander David W. Taylor Naval Ship R&D Center ATTN: Lib Div, Code 522 Bethesda, MD 20084
1	Commander Naval Research Lab ATTN: CODE 2027, Tech Lib Washington, DC 20375
5	Officer-in-Charge Civil Engineering Lab Naval Construction Btn Center ATTN: J. Crawford W. Keenan R. Odello S. Takahashi Dr. W. Shaw Technical Library Port Hueneme, CA 93041
1	Chief of Naval Research Dept of the Navy ATTN: N. Perrone Washington, DC 20360

DISTRIBUTION LIST

No. of Copies	Organization
1	Superintendent Naval Postgraduate School ATTN: Tech Reports Sec Monterey, CA 93940
1	Commander Naval Facilities Engineering Command ATTN: Technical Library Washington, DC 20360
3	Commander Naval Sea Systems Command ATTN: SEA-62R SEA-62Y SEA-9961 Department of the Navy Washington, DC 20360
1	Commander Naval Weapons Evaluation Facility ATTN: Doc Control Kirtland AFB Albuquerque, NM 37117
1	Commander Naval Ammunition Depot ATTN: RD-3 Crane, IN 47522
1	Commandant US Marine Corps Washington, DC 20301
1	Director Development Center, MCDEC/Firepower Division Quantico, VA 22134
1	AFWL/NTES (R. Henny) Kirtland AFB, NM 37117
1	AFWL/NTE, CPT J. Clifford Kirtland AFB, NM 37117
1	AFWL/SUL Kirtland AFB, NM 37117
1	AFELM, The Rand Corporation ATTN: Library-D 1700 Main Street Santa Monica, CA 90406
1	HQ USAF (AFSCAGF) Washington, DC 20330
1	HQ AFSC (SDZ; SDDE; DLAW) Washington, DC 20331
1	RADC (EMTLD/Doc Library) Griffiss AFB, NJ 13441
4	US Army Field Office HQ USAF Systems Command ATTN: SDOA, SDNE DDAB, SDW Andrews AFB Washington, DC 20334
1	ADTC (Tech Lib) Eglin AFB, FL 32542-5000
2	AFATL (DRLRV, J. R. Rutland) (DLYV) Eglin AFB, FL 32542-5000
1	USAFTAWC (OA) Eglin AFB, FL 32542-5000
1	TAC Langley AFB, VA 23365
1	AFAPL (SFH) Wright-Patterson AFB, OH 45433
1	AFFDL (FES) Wright-Patterson AFB, OH 45433
1	AFFDL (FDTR, Dr. Janik) Wright-Patterson AFB, OH 45433

DISTRIBUTION LIST

No. of Copies	Organization
1	AFFDL (FBE, Dr. Bader) Wright-Patterson AFB, OH 45433
1	AFLC (MCNEA) Wright-Patterson AFB, OH 45433
1	AFLC (PPSC) Wright-Patterson AFB, OH 45433
1	AFLC (MMMM) Wright-Patterson AFB, OH 45433
1	AFLC (MEA) Wright-Patterson AFB, OH 45433
1	AFML (LLN, Dr. Nicholas) Wright-Patterson AFB, OH 45433
1	AFIT (Lib Bldg. 640, Area B) Wright-Patterson AFB OH 45433
1	FTD (TD/BTA/Lib) Wright-Patterson AFB, OH 45433
2	Commander-in-Chief Strategic Air Command ATTN: NRI-STINFO Lib Offutt AFB, NB 68113
1	Director Lawerence Livermore Lab Tech Info Div P.O. Box 808 Livermore, CA 94550
2	Director Los Alamos Scientific Lab ATTN: Doc Control for Reports Library C. L. Mader P.O. Box 1663 Los Alamos, NM 87544
2	Director Sandia National Laboratories ATTN: Doc Cont for 3141 Sandia Report Collection L. J. Vortman Albuquerque, NM 87115
1	Director NASA Scientific and Tech Info Facility P.O. Box 8757 BaltWash International Airport, MD 21240
1	Wilfred Baker Engineering 218 E. Edgewood Place San Antonio, TX 78209
1	Aerospace Corporation ATTN: Tech Info Services P.O. Box 92957 Los Angeles, CA 90009
2	Battelle Columbus Lab ATTN: Dr. L. E. Hulbert Tech. Library 505 King Ave Columbus, OH 43201
1	Director Lewis Directorate & Development Lab Lewis Research Center (Mail Stop 77-5) Cleveland, OH 44135
1	Bell Helicopter Textron ATTN: Mr. Nile Fischer P.O. Box 482 Fort Worth, TX 76101
1	The BDM Corporation ATTN: Richard Hensley P.O. Box 9274 Albuquerque International Albuquerque, NM 87119

DISTRIBUTION LIST

No. of Copies	Organization
1	The Boeing Company ATTN: Aerospace Library P.O. Box 3999 Seattle, WA 98124
1	The Boeing Company Vertol Division ATTN: Dave Harding P.O. Box 16858 Philadelphia, PA 19142
1	Goodyear Aerospace Corp ATTN: R. M. Brown, Bldg 1 Shelter Engineering Litchfield Park, AZ 85340
2	Denver Research Institute University of Denver ATTN: Mr. J. Wisotski Technical Library 2390 South University Blvd Denver, CO 80210
1	Fairchild Industries Fairchild Republic Division ATTN: D. Watson Farmingdale LI, NY 11735
2	Falcon Research and Development Company ATTN: L. Mahood A. Stein 109 Inverness Drive Englewood, CO 80112
2	Kaman AviDyne ATTN: Dr. N. P. Hobbs Mr. S. Criscione 33 Second Avenue Northwest Industrial Park Burlington, MA 01803
1	Kaman Sciences Corporation ATTN: Library 1500 Garden of the Gods Road Colorado Springs, CO 80907
1	Kaman-TEMPO ATTN: DASIAC P.O. Drawer QQ, 816 State St Santa Barbara, CA 93102
1	Kaman Tempo ATTN: E. Bryant 715 Shamrock Road Suite UL-1 Bel Air, MD 21014
1	Hughes Helicopters Bldg 5 M/S C303 ATTN: Security Officer Centinela and Teale Sts Culver City, CA 90230
2	University of Delaware Dept of Mech & Aerospace Engineering ATTN: Prof. J. R. Vinson Prof. M. Taya Newark, DE 19711
1	Florida Atlantic Univ Dept of Ocean Eng ATTN: Prof. K. Stevens Boca Raton, FL 33432
1	J.G. Eng Research Associates 3331 Menlo Drive Baltimore, MD 21215
1	Mass Inst Of Tech Aeroelastic & Structures Research Laboratory ATTN: Dr. E. A. Witmer Cambridge, MA 02139
1	Wiedlinger Associates Consulting Eng 110 East 59th Street New York, NY 10022

DISTRIBUTION LIST

No. of Copies	Organization
2	Virginia Polytechnic Inst & State Univ Dept of Eng Mech ATTN: Prof D. Frederick Prof C. J. Smith Blacksburg, VA 24061
1	Brown University Div of Engineering ATTN: Prof. P. Symonds Providence, RI 02912
1	University of Dayton Research Institute ATTN: Dr. S. Bless Dayton, On 45469
1	University of Washington Dept of Aeronautics and Astronautics ATTN: Prof. I. M. Fyfe Seattle, WA 98195
1	Aeronautical Research Associates of Princeton ATTN: Dr. J. W. Leech P.O. Box 2229 50 Washington Road Princeton, NJ 08540
1	New Mexico Institute of Mining & Technology TERA Group Socorro, NM 87801
1	Lockheed Missiles & Space Co. ATTN: J. J. Murphy, Dept. 81-11 Bldg. 154 P.O. Box 504 Sunnyvale, CA 94086
2	McDonnell Douglas Astronautics Company ATTN: Robert W. Halprin Dr. P. Lewis 5301 Bolsa Avenue Huntington Beach, CA 92647
1	The Mitre Corporation ATTN: Library Stop B-150 P.O. Box 208 Bedford, MA 01730
1	Pacific Sierra Research Corp ATTN: Dr. Harold Brode 1456 Cloverfield Boulevard Santa Monica, CA 90404
1	Physics International Corp ATTN: Technical Library 2700 Merced Street San Leandro, CA 94577
4	Carpenter Research Corporation ATTN: Jerry Carpenter J. G. Lewis Technical Library Allan Kuhl P.O. Box 9695 Marina del Rey, CA 90291
1	Science Applications, Inc. ATTN: Technical Library 1250 Prospect Plaza La Jolla, CA 92037
2	Science Applications, Inc. ATTN: Burton S. Chambers John Cockayne P.O. Box 1301 1710 Goodridge Drive McLean, VA 22102
1	Science Systems and Software ATTN: Technical Library P.O. Box 1620 La Jolla, CA 92037
1	S-Cubed ATTN: C. E. Needham P.O. Box 3243 Albuquerque, NM 87108

DISTRIBUTION LIST

No. of Copies	Organization
1	Stanford University ATTN: Dr. D. Bershader Durand Laboratory Stanford, CA 94305
1	SRI International ATTN: Dr. G. R. Abrahamson 333 Ravenswood Avenue Menlo Park, CA 94025
1	Union Carbide Corporation Holifield National Laboratory ATTN: Doc Cont for Tech Lib Civil Defense Research Project P.O. Box X Oak Ridge, TN 37330
1	Washington State University Physics Department ATTN: G. R. Fowles Pullman, WA 99163
2	Southwest Research Inst ATTN: H. N. Abramson A. B. Wenzel P.O. Drawer 28510 San Antonio, TX 78284

Aberdeen Proving Ground

Dir, USAMSAA
ATTN: AMXSY-D
AMXSY-MP, H. Cohen
Cdr, USATECOM
ATTN: AMSTE-TO-F
Cdr, CRDC, AMCCOM
ATTN: SMCCR-RSP-A
SMCCR-MU
SMCCR-SPS-IL